AD 758276

AD

AMMRC CTR 73-6

EROSION-RESISTANT COATING FOR TITANIUM

JANUARY 1973

WILLIAM J. McANALLY, III
Pratt & Whitney Aircraft DIVISION OF UNITED AIRCRAFT CORPORATION
FLORIDA RESEARCH AND DEVELOPMENT CENTER
BOX 2691, WEST PALM BEACH, FLORIDA 33402

Final Report - Contract DAAG46-71-C-0173

D D C
RECEIVED
APR 11 1973
B

Approved for public release; distribution unlimited.

Prepared for

ARMY MATERIALS AND MECHANICS RESEARCH CENTER
Watertown, Massachusetts 02172

NATIONAL TECHNICAL
INFORMATION SERVICE

5 87

Unclassified
Security Classification

DOCUMENT CONTROL DATA - R & D

(Security classification of title, body of abstract and indexing annotation must be entered when the overall report is classified)

1. ORIGINATING ACTIVITY (Corporate author) Pratt & Whitney Aircraft Division of United Aircraft Corp., Florida Research and Development Center West Palm Beach, Florida 33402	2a. REPORT SECURITY CLASSIFICATION Unclassified 2b. GROUP

3. REPORT TITLE

Erosion-Resistant Coating for Titanium

4. DESCRIPTIVE NOTES (Type of report and inclusive dates)

Final Report 30 June 1971 to 30 July 1972

5. AUTHOR(S) (First name, middle initial, last name)

William J. McAnally, III

6. REPORT DATE January 1973	7a. TOTAL NO. OF PAGES ~~89~~ 87	7b. NO. OF REFS 1
8a. CONTRACT OR GRANT NO. DAAG46-71-C-0173 b. PROJECT NO. D/A 1T062105A328 c. AMCMS Code 612105.11.294 Agency Accession No. DA OB 4762	9a. ORIGINATOR'S REPORT NUMBER(S) AMMRC CTR 73-6 9b. OTHER REPORT NO(S) (Any other numbers that may be assigned this report) FR-5243	

10. DISTRIBUTION STATEMENT

Approved for public release; distribution unlimited

11. SUPPLEMENTARY NOTES	12. SPONSORING MILITARY ACTIVITY Army Materials and Mechanics Research Center, Watertown, Massachusetts 02172

13. ABSTRACT

The main objective of this program was to develop the application of TIKOTE®-C on the Ti-6Al-4V alloy with minimum degradation of mechanical properties. The approach for accomplishing this objective was to protect the titanium microstructure with an intermediate nickel barrier, as well as to provide a ductile layer which might inhibit crack propagation. In addition, embrittling effects due to gas absorption during the coating process were minimized by using a lower process temperature. The program was divided into two major categories: (1) TIKOTE-C coating application development by Texas Instruments, Inc., and (2) extensive mechanical tests conducted by Pratt & Whitney Aircraft. A brief evaluation of the fatigue characteristics and erosion resistance of nickel-plated and titanium diboride-coated titanium test specimens was added after the original program was started and hence the data obtained was not as comprehensive as that with TIKOTE-C. Texas Instruments successfully demonstrated the ability to apply a sufficiently uniform coating of TIKOTE-C with good adhesion to wear-sensitive areas on both titanium axial compressor blades and titanium centrifugal impellers from current production engines. TIKOTE-C and titanium diboride coatings on nickel-plated Ti-6Al-4V alloy were found to be 10 to 300 times more erosion resistant than uncoated titanium depending upon test conditions. It was determined that the application of TIKOTE-C to Ti-6Al-4V alloy still caused a severe loss in fatigue strength in spite of the intermediate nickel layer but tensile and creep properties of the base metal were not degraded. However, masking the high stress areas can result in no loss in usable fatigue strength as was demonstrated by applying TIKOTE-C only on the outer half of axial compressor blades to minimize loss of fatigue strength at the blade root. Further evaluation is recommended to demonstrate the effectiveness of the TIKOTE-C erosion-resistant coating in an engine environment by conducting a sand and dust ingestion test with coated titanium compressor rotor components.

DD FORM 1 NOV 65 1473 REPLACES DD FORM 1473, 1 JAN 64, WHICH IS OBSOLETE FOR ARMY USE.

Unclassified
Security Classification

14 KEY WORDS	LINK A ROLE	LINK A WT	LINK B ROLE	LINK B WT	LINK C ROLE	LINK C WT
Titanium Alloys						
Protective Coatings						
Erosion						
Corrosion						
Adhesion						
Fatigue						
Thermal Shock						
Gas Turbine Engines						
Helicopters						

CONTENTS

	PAGE
INTRODUCTION	1
TECHNICAL DISCUSSION	6
CONCLUSIONS AND RECOMMENDATIONS	53
APPENDIX I - Standard Nickel Plating Process on Ti-6Al-4V STR 109979 Texas Instruments, Incorporated	54
APPENDIX II - Listing of Erosion Coating Runs	56
APPENDIX III - Method of Determining Coating Adhesion Bond Strength in Shear	69
APPENDIX IV - Method for Determining Coating Adhesion Bond Strength in Tension	71
APPENDIX V - Method for Determining the Effects of Hot Salt Stress Corrosion on Titanium Alloys	75

Preceding page blank

LIST OF ILLUSTRATIONS

Figure		Page
1	Helicopters Operating From an Unimproved Landing Site	2
2	Typical Fixed-Wing Aircraft Operation on a Remote Landing Strip	2
3	Typical Compressor Erosion Damage	3
4	State-of-the-Art - 1970	4
5	Erosion-Resistant Coating for Titanium Program Schedule	5
6	Coating Thickness of PT6 Blade	8
7	JT8D Blade Coating Distribution	9
8	Equipment Used for Coating Centrifugal Impellers	10
9	Results of Impeller Heating Tests With Pancake Coils and Outside Solenoid	10
10	Thickness of Erosion Coating on Impeller No. 6	10
11	Process Outline for Application of TIKOTE® -C Titanium	11
12	Flat Fatigue Bar Test Specimen Gage Section Normally Glass Bead Peened. For Masked Gage, Only Area A Was Coated	12
13	Preliminary Fatigue Results of Tests at Texas Instruments	13
14	Load vs Deflection for TIKOTE® -C Coated Fatigue Specimens	15
15	Power Factor and Frequency vs Flexure Cycles During Fatigue Testing of TIKOTE® -C Coated Specimens	15
16	Microstructure and Hardness Traverse of Blade and Impeller	16
17	Electron Beam Scan of TIKOTE® -C on Titanium JT8D Blade Compared to Visual Photomicrograph	18
18	Cracks in TIKOTE® -C Coated Fatigue Specimens With 2- and 5-mil Nickel Plate	19

LIST OF ILLUSTRATIONS (Continued)

Figure		Page
19	Specimens Used to Evaluate Adhesion Strength	23
20	Typical Specimen After Peening Test	23
21	Thermal Shock Tubular Specimens	25
22	Test Setup Schematic for Repeated Thermal Shock Testing	26
23	Hot Salt Stress Corrosion Specimens	27
24	Specimens Used to Evaluate Erosion Resistance	29
25	SS White Abrasive Unit, Temperature Controls and Readout	30
26	Tensile Test Specimens	32
27	Creep Specimens	35
28	Rotating Beam Fatigue Test Specimens	36
29	Reverse-Bending, High-Cycle Fatigue Results at Room Temperature	39
30	Reverse-Bending, High-Cycle Fatigue Results at 900°F	39
31	Typical JT8D 6th-Stage Axial Compressor Blades Showing the Three Different Types of Surface Treatments	40
32	Typical Stresscoat Patterns and Strain Gage Locations in First Bending Mode of Vibration	41
33	JT8D 6th-Stage Blade Stress vs Cycles to Failure	44
34	Masked JT8D Blade Showing Location of Failure Origin at Edge of TIKOTE® -C	45
35	JT8D Blade Showing Location of Failure Resulting From TIKOTE® -C Overflow Onto the Masked Portion of the Airfoil	46
36	Typical Failure in the Uncoated Region of JT8D Masked Blades	47
37	Photomicrographs of PT6 A-27 Impeller Coated With TIKOTE® -C	49

LIST OF ILLUSTRATIONS (Continued)

Figure		Page
38	Cross Sections of JT8D Axial Compressor Blade Showing Thickness of TIKOTE® -C	50
39	Photomicrograph of JT8D 6th-Stage Compressor Blade Showing Voids at the Titanium/Nickel Interface	51
40	Photomicrographs of JT8D 6th-Stage Compressor Blades Showing Microstructure Changes	52

LIST OF TABLES

Table		Page
I	Properties of TIKOTE-C - Ti_2CN	6
II	Properties of Single Crystal or Hot-Pressed TiB_2	20
III	List of Tests Performed by P&WA Under AMMRC Contract DAAG46-71-C-0173	21
IV	Adhesion in Shear	24
V	Adhesion in Tension	24
VI	Erosion Data for Two Coating Systems on Ti-6Al-4V Alloy	31
VII	Erosion Resistance of Coatings on Ti-6Al-4V Relative to Uncoated Ti-6Al-4V	32
VIII	Room Temperature Tensile Properties	33
IX	900°F Tensile Properties	34
X	900°F Creep Properties	35
XI	Room Temperature Rotating Beam Fatigue Results	37
XII	Rotating Beam Fatigue Results at 900°F	38
XIII	Fatigue Data - JT8D 6th-Stage Axial Compressor Blade, P/N 571206, Tested at Room Temperature in First Bending Mode	42

NOMENCLATURE

KHN	Knoop Hardness Number
mil	0.001 in.
μ	Micron, meter x 10^{-6}
μin.	Microinch
VHN	Vickers Hardness Number
TE	Trailing Edge
LE	Leading Edge
MRT	Maximum Root Thickness
TEM	Trailing Edge at Masking Line
TED	Trailing Edge at Overrun

INTRODUCTION

Gas turbine engines require high airflow per horsepower, and thus are vulnerable to degradation caused by erosive particle contaminants in the air. When subjected to such contamination, degradation is evidenced by loss of power, loss of surge margin, and increased specific fuel consumption because of either erosion or fouling of precision airfoil sections in the compressor and turbine. Most of the early gas-turbine-engine erosion experience was obtained with fixed-wing aircraft operating from paved runways, and particle ingestion was not a significant problem. Tactical helicopter and fixed-wing aircraft operations from unimproved landing sites, however, forced a reappraisal of the vulnerability of gas turbines to solid-particle ingestion. Figure 1 shows helicopters operating under these adverse conditions, and Figure 2 shows a fixed-wing aircraft operating in the same type of environment. Premature engine removals, because of resultant erosion damage, drastically reduced the time between overhaul, in some instances by a factor of 10 or more. Generally, when the engines were overhauled, all compressor components had to be replaced. Examples of typical axial and centrifugal compressor damage are shown in Figure 3.

Two approaches to solving the problem were apparent: (1) remove the particles from the airstream, and/or (2) make the engines more erosion-resistant. Because the need was urgent and the particle-removal approach was best suited to quick implementation, this course was adopted by most helicopter engine and airframe manufacturers. As a result, virtually all helicopters now operating in Southeast Asia have some form of sand and dust particle separation system. However, in gas-turbine-powered, fixed-wing aircraft, it is not feasible to fit effective inlet protection devices; and even with inlet protection devices installed in helicopters, erosion of compressor blades, stators, and impellers continues to occur at a reduced rate because separators do not remove fine particles. Hence, there is still a critical need to make engines more erosion resistant.

Concern over the problem of metal erosion because of sand and dust ingestion prompted P&WA™ to undertake a laboratory test program in 1968 to investigate the phenomenon. Comparative erosion tests were conducted on Ti-6Al-4V and a variety of other structural alloys. Subsequently, potential erosion-resistant coatings were evaluated for erosion resistance, smoothness, adhesion, and effect on base material metallurgical characteristics. The results indicated that Texas Instruments' TIKOTE®-C titanium carbonitride coating and the United Aircraft Research Laboratories' titanium diboride coating were superior to the coatings evaluated and could provide 10 to 100 times more erosion resistance than bare Ti-6Al-4V.

Figure 1. Helicopters Operating From an Unimproved Landing Site. FC 26821

Figure 2. Typical Fixed-Wing Aircraft Operation on a Remote Landing Strip. FC 27741

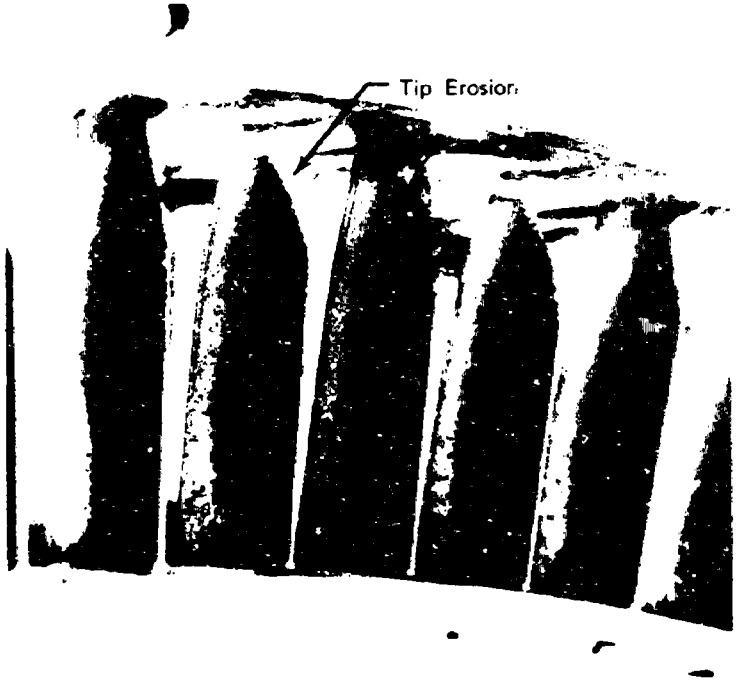

XP 65094

Axial Compressors

FE 90374

Centrifugal Impellers

Figure 3. Typical Compressor Erosion Damage

FD 64883

Prior to initiating this program, an earlier investigation[1] had reported a severe loss in fatigue strength when TIKOTE-C was applied to Ti-6Al-4V. At that time, this was attributed to alpha-case surface embrittlement due to the absorption of oxygen, carbon, and nitrogen during the coating process, as shown in Figure 4. The main objective of the program reported herein was to overcome earlier contamination problems and develop the application of TIKOTE-C on Ti-6Al-4V alloy with minimum degradation of mechanical properties. The approach for accomplishing this objective was to protect the titanium microstructure with an intermediate nickel barrier, as well as to provide a ductile layer that might inhibit crack propagation. In addition, embrittling effects due to gas absorption during the coating process were minimized by reducing the process temperature from 1800°F to 1200°F. An additional objective of this program was to briefly evaluate fatigue characteristics and erosion resistance of nickel-plated titanium test specimens with a titanium diboride coating applied by United Aircraft Research Laboratories.

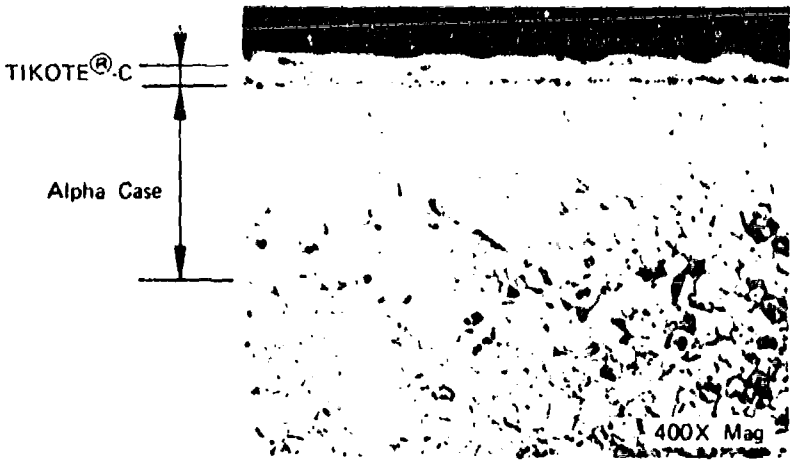

Figure 4. State-of-the-Art - 1970. FD 64885

Since the application of TIKOTE-C on steel compressor components had been successfully demonstrated as part of the Allison T-56 component improvement program under Air Force Contracts F33657-70-C-0712 and F33657-71-C-0341, the majority of the effort under this program was concentrated on evaluating TIKOTE-C instead of titanium diboride. The application of titanium diboride was still in the laboratory research stage. As shown in the program schedule (Figure 5), this program involved a 10-month subcontract with Texas Instruments, Inc., to develop the application of their TIKOTE-C erosion resistant coating. At its conclusion, Pratt & Whitney Aircraft performed laboratory tests, over a range of temperatures up to 900°F, to measure the erosion resistance of the coating and its effect on mechanical properties and corrosion susceptibility of Ti-6Al-4V.

The technical discussion of the program is divided into three sections: (1) TIKOTE-C coating application development by Texas Instruments, Inc., (2) Titanium Diboride plating by United Aircraft Research Laboratories, and (3) mechanical tests conducted by Pratt & Whitney Aircraft.

---

[1]Green, H. M., Manufacturing Techniques for Application of Erosion Resistant Coatings to Turbine Engine Compressor Components, General Electric Company; Technical Report No. AFML-TR-70-114, Air Force Systems Command, United States Air Force, Wright-Patterson Air Force Base, Ohio, May 1970.

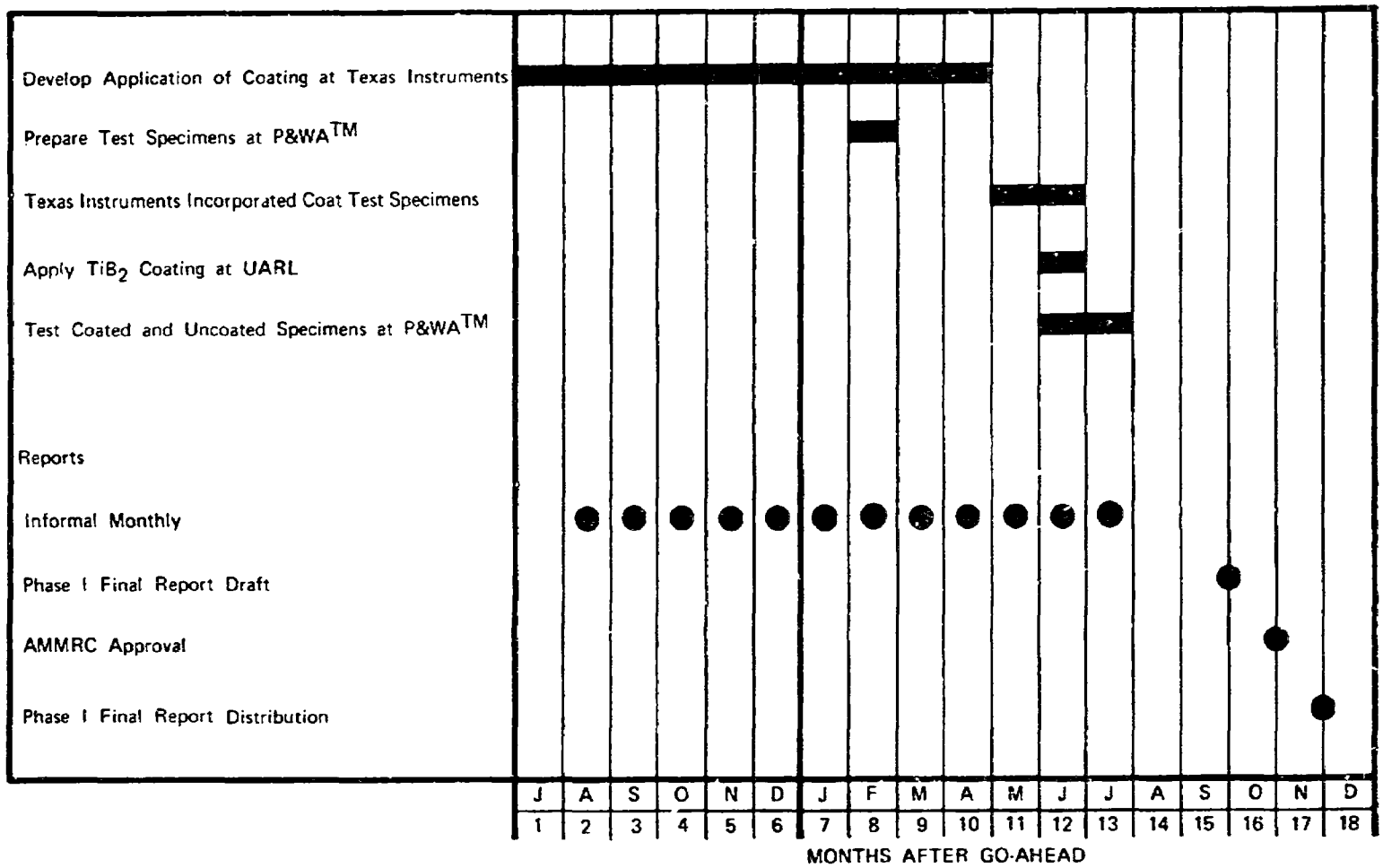

Figure 5. Erosion-Resistant Coating for Titanium Program Schedule. FD 64884

TECHNICAL DISCUSSION

I. TEXAS INSTRUMENTS, INC. - TIKOTE-C

TIKOTE-C is a proprietary titanium carbonitride overlay coating, applied by a chemical vapor deposition process that is basically a reduction of metal halides in a hydrogen atmosphere. In developing the coating, nitrogen was added to titanium carbide to increase the strain capability of the coating and reduce the modulus of elasticity somewhat from 58 to 50 million psi. Some other properties of TIKOTE-C are listed in Table I.

TABLE I. PROPERTIES OF TIKOTE-C - Ti_2CN

Melting Point, °F	5790
Density, lb/in^3	0.185
Specific Heat, Btu/lb/°F	0.130
Thermal Conductivity, Btu/hr/ft/°F	12.7
Coefficient of Thermal Expansion, per °F	5.5×10^{-6}
Hardness, KHN	2400

A program was conducted by Texas Instruments, Inc., to demonstrate the application of approximately 0.001 in. of TIKOTE-C on nickel-plated titanium alloy engine components. Laboratory test specimens, JT8D 6th-stage blades, PT6 1st-stage blades, and PT6 centrifugal impellers were supplied by Pratt & Whitney Aircraft for coating to determine the degree of success in accomplishing the program objectives. Evaluations by Texas Instruments showed a loss in fatigue strength in highly stressed coated areas, but otherwise generally favorable results were obtained with respect to adhesion, coverage, protection, masking, and other mechanical properties. Coating adhesion was apparently controlled by the quality of the nickel plating, and coating thickness was controlled by uniformity of the specimen temperature profile. Masking techniques permitted retention of fatigue strength on partially coated components. The equipment used to coat the test samples and axial compressor blades was a standard unit used for coating steel blades, while a special unit was built for coating centrifugal impellers.

Nickel-Plating Process

Standard Nickel Plating Process

Several experimental plating procedures and vacuum bonding bake cycles were tried to optimize the nickel plate as a bonding and ductile protective interlayer for the coating. The final procedure adopted as a standard is described in Appendix I. It consists of ammoniacal electroless nickel-phosphorous using an alkaline bath, followed by two layers of sulfamate electrolytic nickel, with an intermediate vacuum bonding bake cycle. Approximately 250 μin. of nickel were applied; lesser amounts would reduce TIKOTE-C adhesion to the nickel.

The effectiveness of this bonding procedure has been illustrated by the fact that deletion of the nickel plating prevents coating adhesion on specific areas. This procedure worked completely, except for some spotting on masked JT8D blades. (However, this failure may have been related to the accidental overheating of some of the blades prior to coating deposition or to a partial lifting of the masking allowing some trace deposition of nickel.)

The deficiencies that were noted in the nickel-plating procedure were (1) the occasional development of blisters and spalling and (2) controlling plating thickness on sharp corners and in recesses. A rework procedure for the plated parts was not developed, and attempts to strip the nickel made some parts unusable.

Other Nickel-Plating Techniques

The application of a nickel interlayer was evaluated using sputtering techniques to obtain minimum changes in the microstructure of the substrate. The process has the advantage of being significantly cleaner than aqueous-solution plating processes. Attempts to apply the nickel to blade shapes were not successful, apparently due to geometric effects. This technique was not pursued because of the requirement for plating the substantially more complex shape of a centrifugal impeller.

Attempts were made to develop an all electroless nickel-plating process that possessed good adhesion between the nickel and TIKOTE-C interface. Poor TIKOTE-C adhesion resulted with just the electroless nickel-phosphorous (8-10%) plate using an alkaline bath, so a borane electroless nickel overlay was evaluated. Satisfactory nickel to titanium adhesion was obtained by the application of 50 μin. of electroless nickel-phosphorous, followed by 150 to 200 μin. of borane electroless nickel. The 1200°F vacuum bonding heattreat was used, resulting in an adherent nickel plate. However, attempts to coat this borane electroless nickel surface with TIKOTE-C were entirely unsuccessful. Lack of bonding was attributed to the 1 to 5% boron content of the nickel plate.

An electroless nickel process would be highly preferable for the elimination of geometrical restrictions of the electrolytic process and requirement for conforming anodes, but maximum adhesion of TIKOTE-C to nickel could only be obtained with the electrolytic process.

Coating Equipment

The blades and laboratory test specimens were coated in a standard laboratory reactor that was modified to (1) improve gas sealing to the end plates, (2) provide continuous temperature measurement throughout the run, (3) incorporate an automatic control for sequencing the operations of the coating cycle, and (4) add purifiers on the reactant gas supply lines. The reactor was operated only for titanium during the 10-month span of coating and experimenting to minimize any contamination from the steel coating process.

The heating of each different sample shape required modifications to the induction heating setup. While most regularly shaped samples with thick cross sections could be uniformly heated with induction heating, the heating profile of short, thin samples and blades often was not as uniform as desired. Low-aspect-ratio PT6 1st-stage blades were finally coated using a thermal profile that does provide the majority of the coating in the erosion area of that particular blade, i.e., the leading edge near the root, as illustrated in Figure 6.

However, this nonuniformity of the thermal profile resulted in a decision to use a blade with a higher aspect ratio to facilitate the demonstration of applying the coating uniformly; thus, longer 6th-stage JT8D blades were also studied. The JT8D blades were selected because the JT8D engine is a current production engine, and new and used blades were readily available; however, it should be noted that they are not generally subject to sand and dust erosion, since the engines are used mostly in commercial airliners.

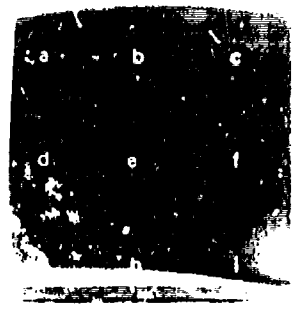

TE	LE		Coating Thickness, in. x 10^{-3} Concave	Convex
0.3	1.5	a	0.5	0.4
		b	0.6	0.6
		c	0.7	0.7
0.2	2.5	d	0.5	0.5
		e	0.7	0.6
		f	0.9	0.7
0.3	2.8	g	0.8	0.8
		h	1.3	1.1
		i	1.5	1.3

Figure 6. Coating Thickness on PT6 Blade. FD 65123

Additional modifications to the blade induction heating setup resulted in an improved thermal profile, and the resultant JT8D blade coating uniformity was improved over that of the PT6 blade, as can be noted in Figure 7. Coating thickness distribution for a root-masked JT8D blade is also included in Figure 7.

The size and shape of the PT6 engine impellers were such that it was not possible to coat them in the 6-in. diameter blade/sample reactor. A reactor system previously used to coat 18-in. diameter vane and shroud assemblies was modified to coat the 9.5-in. diameter impellers (Figure 8). Extensive manipulation of induction coil designs was required to provide an acceptable thermal profile and resultant acceptable coating thickness distribution. The "best" coil design yielded the temperature profile shown in Figure 9 and was used to apply TIKOTE-C to impellers shipped under the contract. The coating thickness distribution obtained on the PT6 impellers is shown in Figure 10.

Coating Application and Masking

The application of TIKOTE-C at 1200°F and the makeup of the coating constituents were standardized under the previously mentioned Air Force contracts for steel compressor components, and the same process was used for this program. The entire procedure for applying TIKOTE-C on titanium, including nickel plating, is outlined in Figure 11. This represents the current "best" procedure, though many possibilities exist for optimization and improvement. All the experimental and final coating runs are listed in Appendix II.

The conventional masking technique (steel parts) was to apply a thin coating of aquadag (colloidal graphite in H_2O) by brushing or dipping. After the coating procedure has been completed, a light glass bead cleanup was used to remove the unwanted coating from the masked surfaces. However, with titanium parts it was observed that some interaction occurs between the graphite and the surface of titanium during the coating run. Since it was determined that the nickel plating served as a bonding layer among other functions, the ability to prevent TIKOTE-C adhesion on specific areas by omission of the nickel layer was demonstrated. This "no nickel" masking technique for preventing TIKOTE-C adhesion has proven very successful on a large number of Pratt & Whitney Aircraft samples and blades, with the exception described earlier, where some coating remained in the root area on the masked JT8D blades.

FE 122496

A. Entire Blade

LE		Coating Thickness, in. x 10^{-3} Concave	Convex
0.7	a	0.4	0.4
	b	0.4	0.4
	c	0.5	0.4
1.2	d	0.7	0.8
	e	0.9	0.8
	f	1.1	1.0
1.0	g	0.7	0.8
	h	0.9	0.9
	i	0.9	1.0
0.9	j	0.7	0.6
	k	1.0	0.9
	l	0.9	0.9

FE 117557

B. Masked Root

LE		Coating Thickness, in. x 10^{-3} Concave	Convex
1.8	a	2.9	1.0
	b	0.9	1.0
	c	1.9	1.1
1.4	d	1.2	0.95
	e	1.1	1.0
	f	1.3	1.1
1.1	g	1.0	0.8
	h	1.1	1.0
	i	1.2	1.0
	j	0.9	0.7
	k	1.2	1.0
	l	1.2	1.0

Figure 7. JT8D Blade Coating Distribution. FD 65122

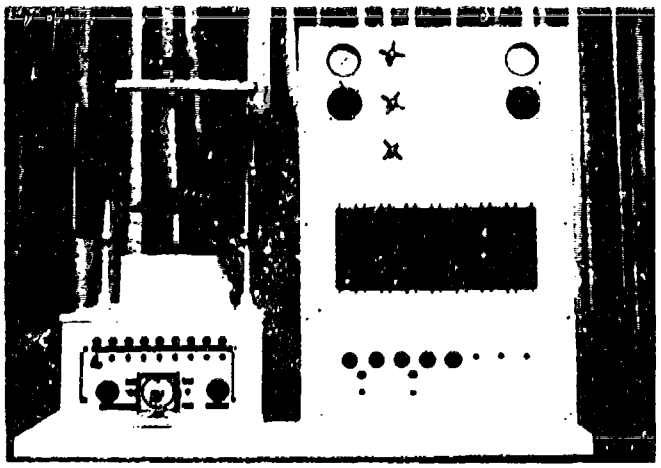

Figure 8. Equipment Used for Coating Centrifugal Impellers. FE 122450

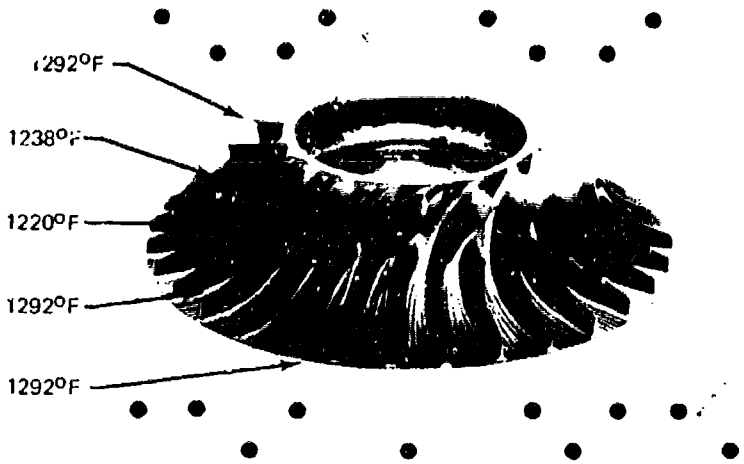

Figure 9. Results of Impeller Heating Tests With Pancake Coils and Outside Solenoid. FD 65112

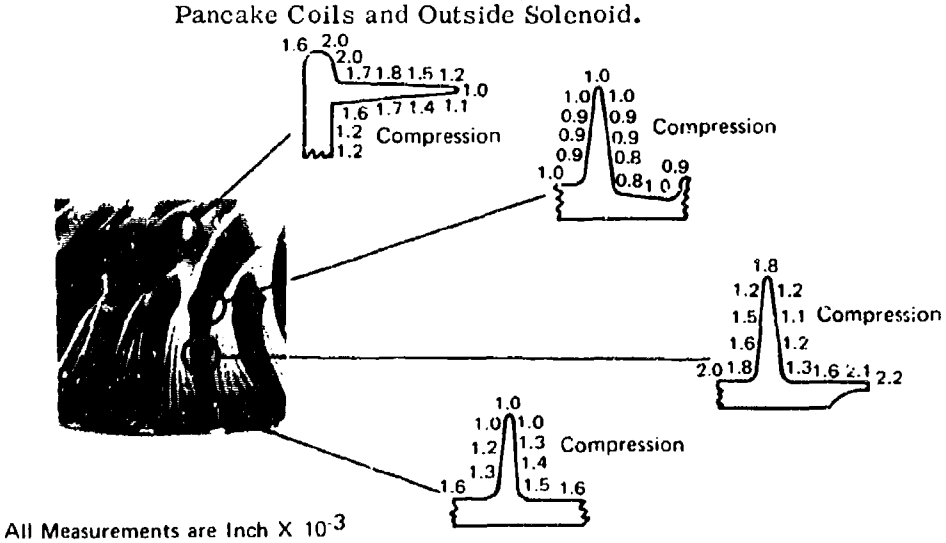

Figure 10. Thickness of Erosion Coating on Impeller No. 6. FD 65113

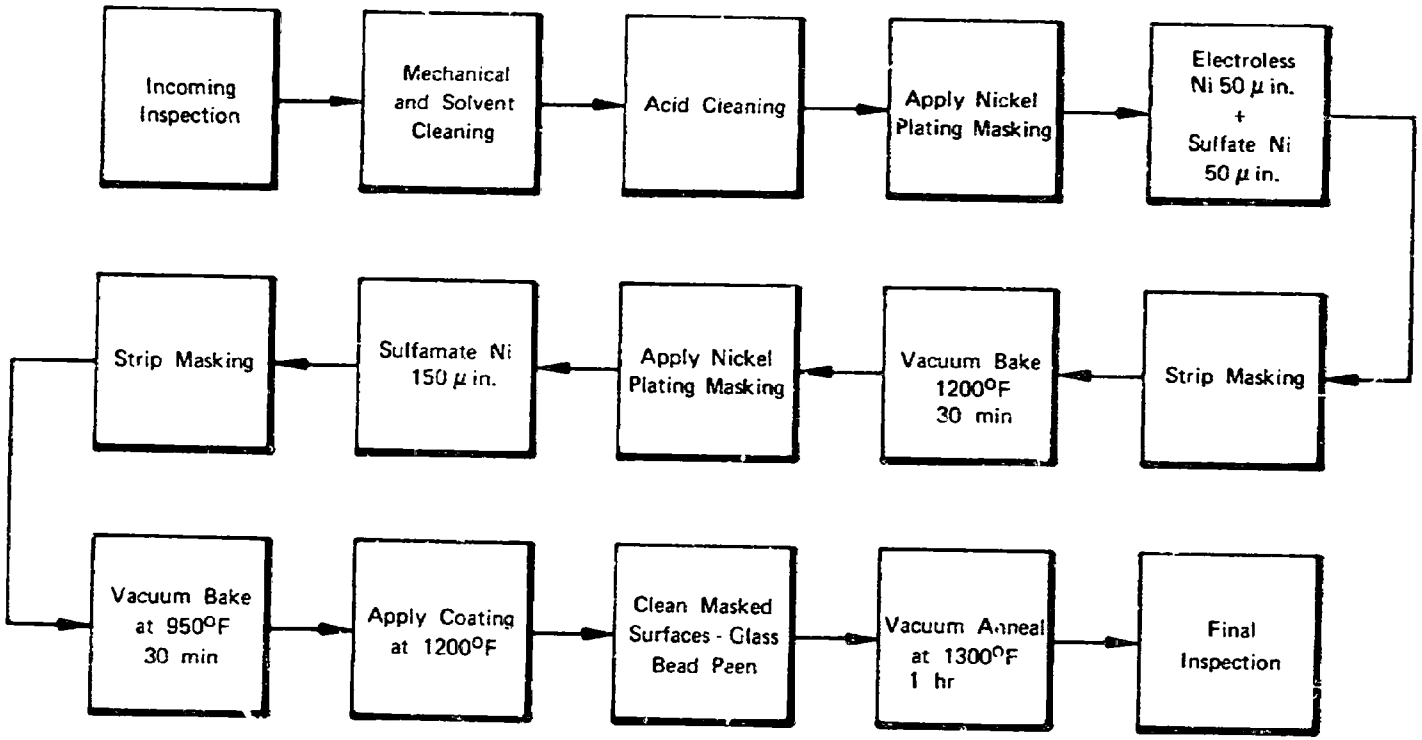

Figure 11. Process Outline for Application of TIKOTE® -C on Titanium.

FD 65114

Evaluation

Fatigue

Preliminary measurement of the fatigue strength of coated laboratory specimens was made by Texas Instruments using the flat configuration shown in Figure 12.

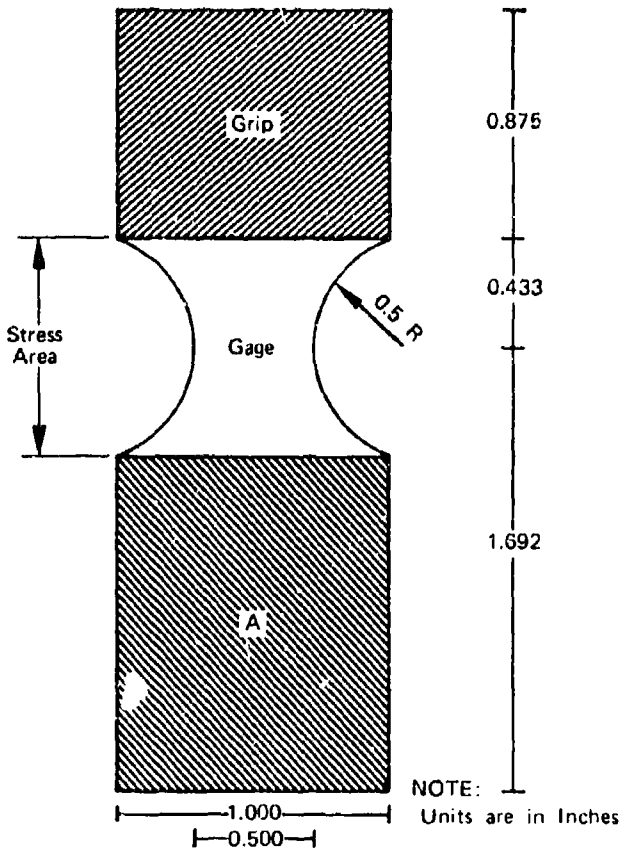

Figure 12. Flat Fatigue Bar Test Specimen Gage Section Normally Glass Bead Peened. For Masked Gage, Only Area A Was Coated. FD 65115

One end is mounted in a vise on a vibrating electromagnet head, leaving the other end to oscillate freely. Measurement of the cross section of the gage area and the load vs deflection for each sample permitted the maximum surface stress to be calculated by standard formulas. The actual test was conducted by adjusting the vibrating frequency to the first resonance mode and adjusting the amplitude, as-measured through a graduated telescope, to produce the desired stress level. The vibration was continued until fracture or runout occurred. The six series of tests conducted are listed below:

1. As-received titanium

2. Coated stress area (standard Ni, includes 50μin. electroless Ni)

3. Masked stress area (sputtered Ni)

4. Masked stress area (standard Ni, includes 50μin. electroless Ni)

5. Coated stress area (2-mil Ni, includes 50μin. electroless Ni)

6. Coated stress area (5-mil Ni, includes 50μin. electroless Ni)

The data are plotted in Figure 13, and conclusions from these tests were:

1. Masking of the stressed area results in retention of essentially all of the original fatigue strength.

2. Coating in the stress area decreased the fatigue strength by 58%.

3. Samples with thicker nickel showed further decreases in fatigue strength.

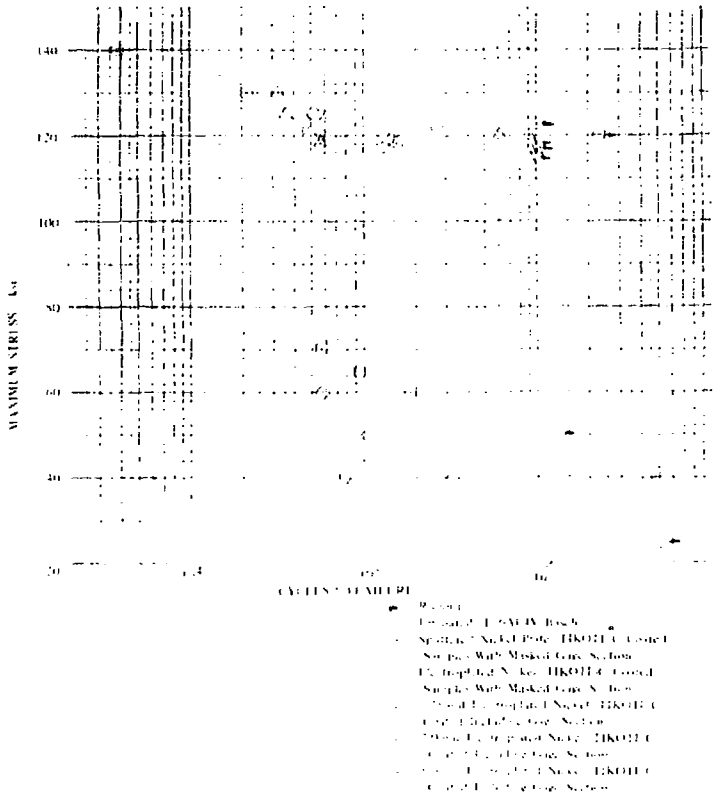

Figure 13. Preliminary Fatigue Results of Tests at Texas Instruments. DF 92816

The data from test series having coated stress areas are based on calculations utilizing the modulus of elasticity of titanium. However, since the maximum stress occurs at the surface, and the surface is really a ceramic with a modulus three times the value assumed in the calculation, the true stress in the coated surface is around three times the calculated stress. This means that the maximum surface stress at the fatigue limit is approximately 150K psi; not an unreasonable value for ceramic films.

Fatigue strength measurements of TIKOTE-C on thicker nickel plating were observed to lower the fatigue strength even more than the standard minimum thickness and also failed in a slightly different mode. It was noted that the power level required to maintain a desired amplitude of flexure decreased during the test, suggesting a work hardening of the nickel layers. The greater decrease in fatigue strength with thick nickel underlayers could be caused by the low fatigue strength of the nickel.

(Note: Pratt & Whitney Aircraft has experienced fatigue strength losses of as much as 30% at room temperature and elevated temperatures on titanium plated with either electrolytic nickel or chromium. The fatigue strength losses were directly proportional to plate thickness.)

The cause of changes in frequency and power that were observed during the fatigue testing of the TIKOTE-C-coated fatigue specimens with thicker nickel plating was determined to be yielding of the annealed nickel plate. Load vs deflection curves for the three types of coated fatigue specimens are given in Figure 14. The fatigue specimen with 5-mil nickel plating sustained an 8-mil permanent deflection when loaded to a calculated stress level of 30,000 psi. The 2-mil nickel plated specimen sustained a 4-mil permanent deflection under the same stress loading, while the fatigue specimen with the standard 0.25-mil nickel plating was completely elastic. The degree of permanent set was reversible and caused a hysteresis loop when flexed in both directions. This cold working of the thicker nickel plating could explain the observed decreasing power required to fatigue those specimens as shown in Figure 15. Also, the frequency of the samples remained relatively constant until a surface crack probably occurred. This was relatively early in the case of the 5-mil nickel plated specimens, and the subsequent gradual failure may be the result of a crack inhibiting effect in the ductile nickel layer.

Coating Uniformity

The program goal of a 1-mil coating over all surfaces of components was not achieved without excessive coating in some surface areas. The components generally do have the desired coating thickness in areas subject to erosion and are expected to provide the required protection. The coating thickness appeared to be dictated by the ability to establish a uniform thermal profile on any component.

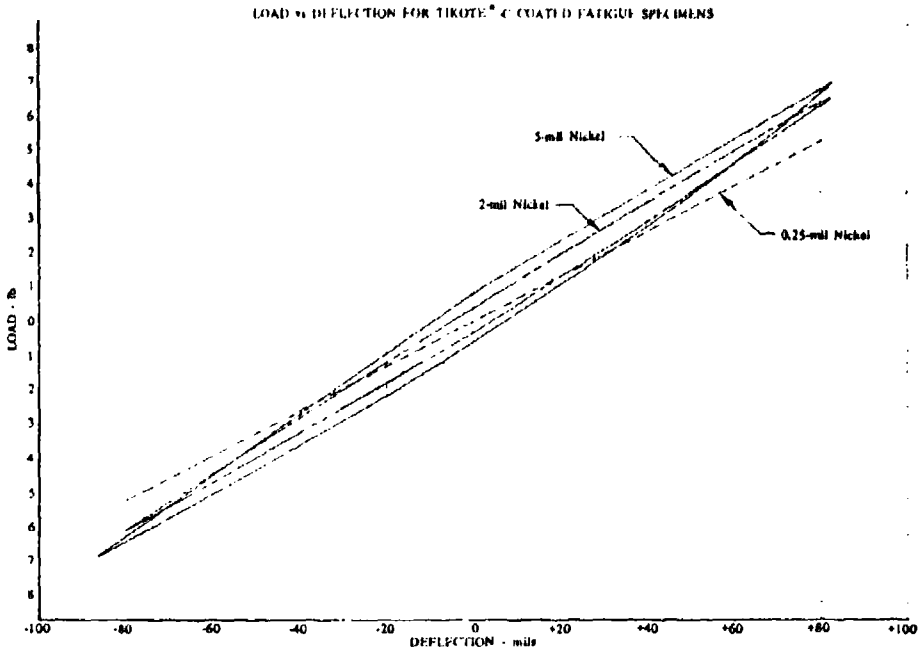

Figure 14. Load vs Deflection for TIKOTE®-C Coated Fatigue Specimens. DF 94721

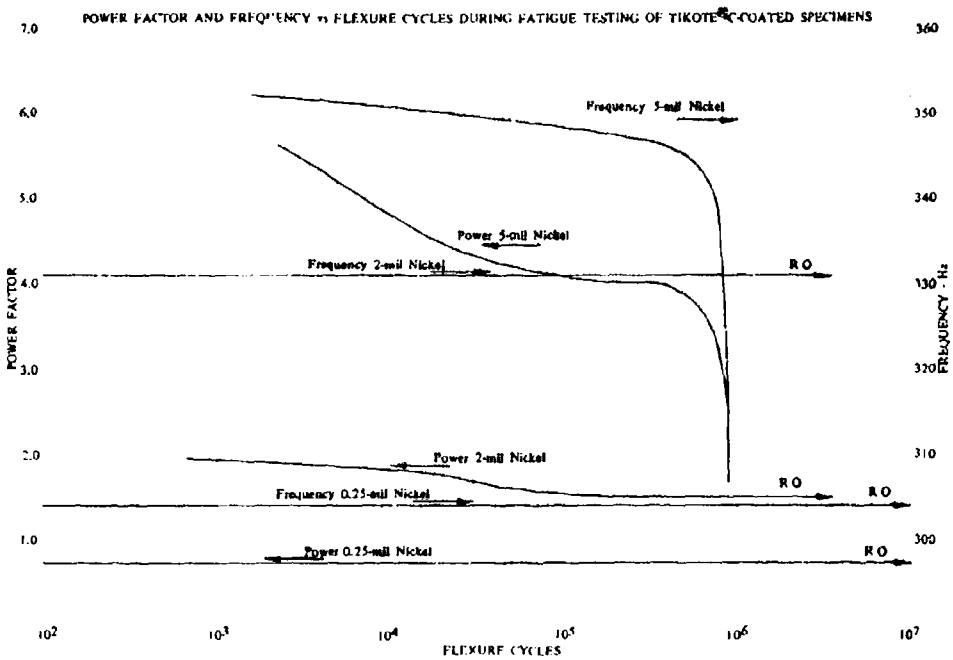

Figure 15. Power Factor and Frequency vs Flexure Cycles During Fatigue Testing of TIKOTE®-C Coated Specimens. DF 94722

Metallographic Analysis

Photomicrographs of the microstructure of a coated JT8D blade and PT6 impeller are shown in Figure 16. Minimum diffusion of the original nickel plate into the titanium was observed; the intermetallic layers formed were only about twice the original 0.00025-in. nickel thickness. The core microstructure of the titanium was normal for a well-annealed component. The results of microhardness traverse samples, also shown in Figure 16, indicate that little increase in hardness was encountered during processing, and confirms minimum change to the microstructure.

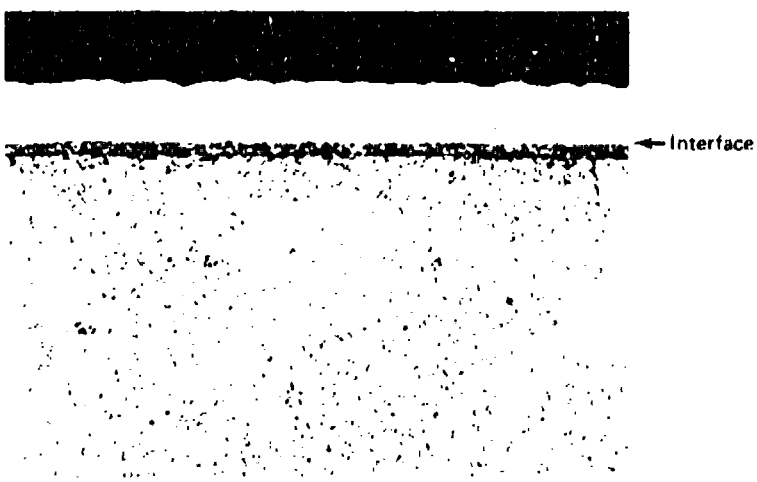

JT8D Blade - Masked

Distance From Interface, in.	KHN_{200}
0.0005	417
0.001	394
0.002	402
0.003	387
0.004	358
0.012	366

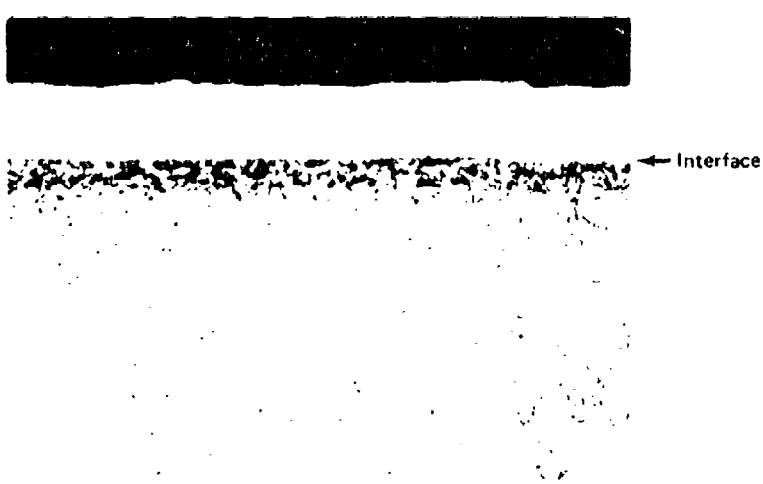

PT6 Impeller - No. 6

Distance From Interface, in.	KHN_{200}
0.0005	386
0.001	345
0.002	378
0.003	402
0.004	345
0.012	358

Figure 16. Microstructure and Hardness Traverse of Blade and Impeller FD 65116

An electron beam scan analysis was conducted on a cross section of TIKOTE-C coating on a JT8D blade. The results and visual photomicrographs are shown in Figure 17. The analysis shows that aluminum, vanadium, and phosphorous remain in their original position with little diffusion. Nickel is observed to form intermetallics and to diffuse into the substrate. A profile count of the layers suggests that the gray layer closest to the substrate is Ti_2Ni and the lighter layer next to the coating is $TiNi_3$. For this typical sample, no pure nickel is apparent.

Failed fatigue test specimens were examined to evaluate the concept of retardation of crack propagation by the ductile layer of nickel plate. In cross sections taken normal to the fatigue cracks, all observed cracks had propagated through the TIKOTE-C coating, nickel, intermetallics, and into the titanium. Photomicrographs of cross sections of TIKOTE-C-coated fatigue specimens with 2-mil and 5-mil nickel plate are shown in Figure 18. Cracks are readily visible through the nickel plating, intermetallics and into the titanium substrate. On the 2-mil nickel specimen, it can be seen that 1.2-mil layer of pure nickel remains and that on the 5-mil nickel specimen 3.5-mils of pure nickel remains.

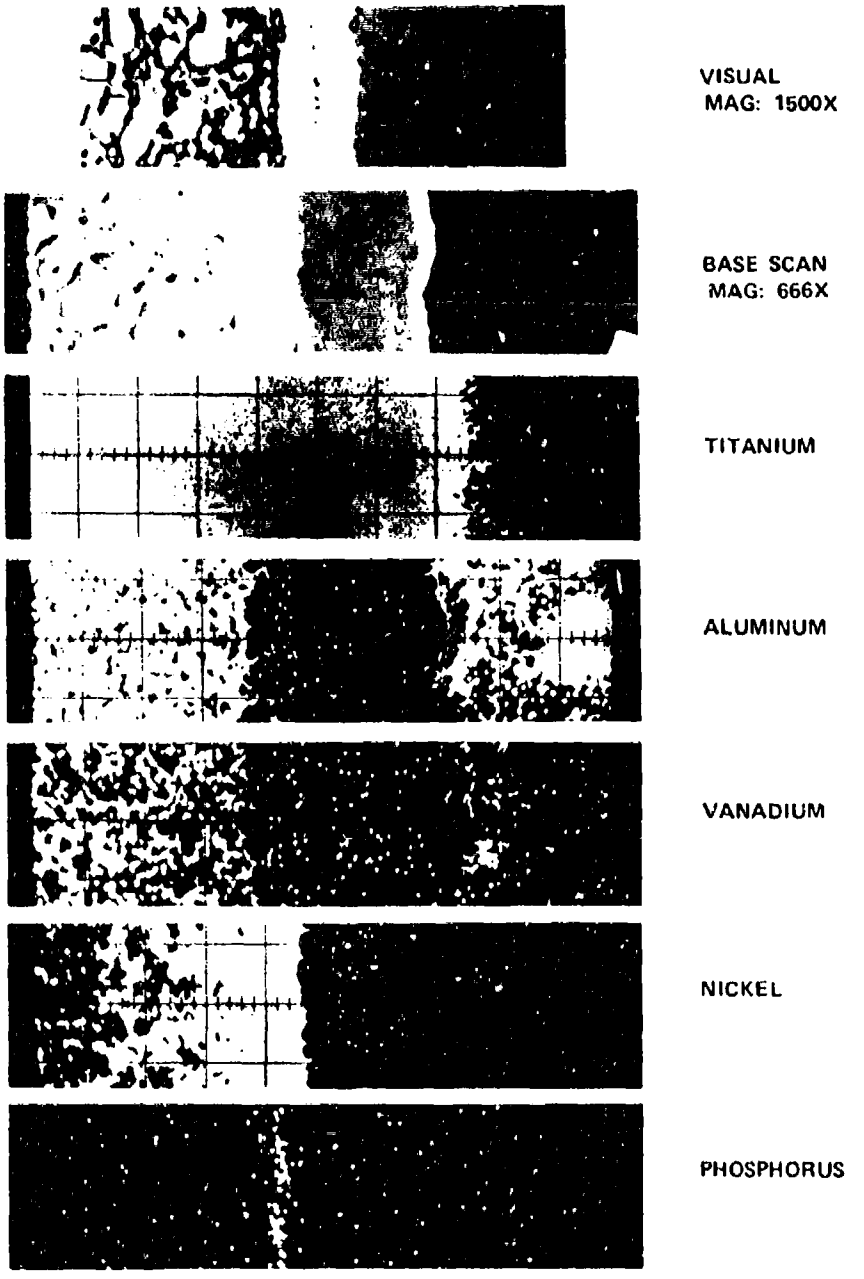

Figure 17. Electron Beam Scan of TIKOTE[R]-C on Titanium JT8D Blade Compared to Visual Photomicrograph

FD 67142

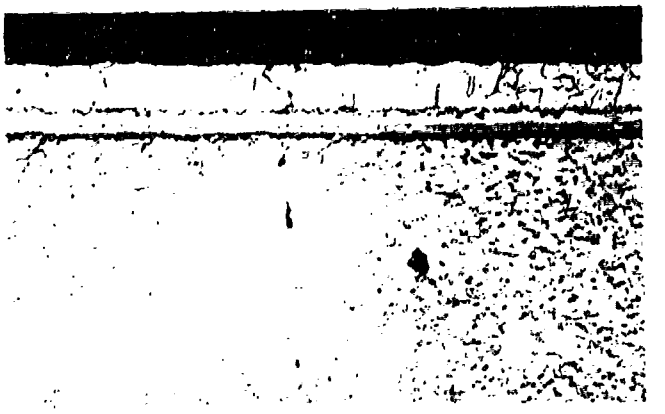

2-mil NICKEL

MAG: 250X

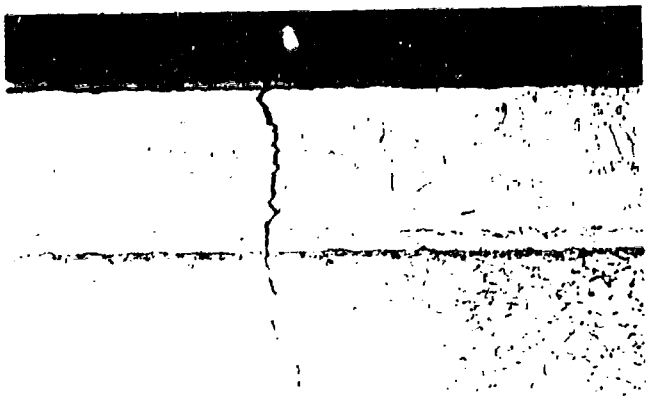

5-mil NICKEL

MAG: 250X

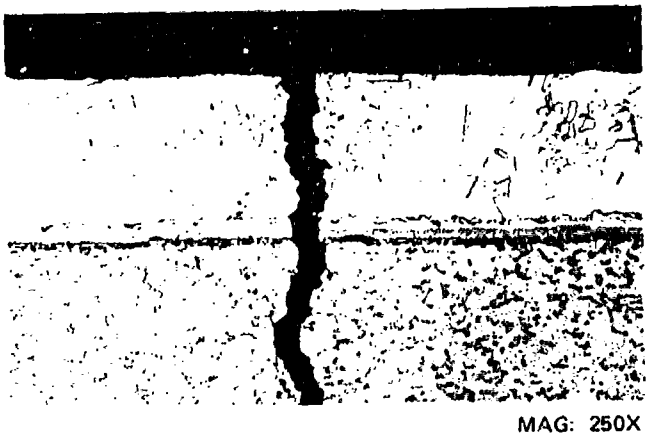

5-mil NICKEL

MAG: 250X

Figure 18. Cracks in TIKOTE[R]-C-Coated Fatigue Specimens With 2- and 5-mil Nickel Plate

FD 67143

II. UNITED AIRCRAFT RESEARCH LABORATORIES - TITANIUM DIBORIDE

United Aircraft Research Laboratories (UARL) plates titanium diboride from a fused salt bath at 1200°F. Excellent adhesion has been obtained on steel, tungsten, niobium, nickel, molybdenum, and graphite, at thicknesses up to 0.035-in. Titanium is first plated with nickel and then plated with TiB_2 with excellent results.

Plating speeds possible in the UARL TiB_2 electrodeposition process can be as high as 6 mil/hr. At this rate, a protective coating of 0.5 mil would take 5 min. Electroplating lends itself well to scaling up, since only a larger salt bath and furnace are required, however, means must be provided to protect the salt bath from air and moisture contamination when changing electrodes and during plating.

Microhardness measurements using a Reichert microhardness tester at 84 gms load indicated a hardness of 4060 ± 200 VHN. The same operator on the same apparatus obtained a value of 3027 ± 150 VHN for boron, which is identical to the values reported in the literature for vapor-deposited boron. Thus, the value of over 4000 VHN for UARL electrodeposited TiB_2 represents a hardness second only to diamond.

Some other properties of TiB_2 given in the literature are listed in Table II.

TABLE II. PROPERTIES OF SINGLE CRYSTAL OR HOT-PRESSED TiB_2

Melting Point, °F	5700
Density, lb/in^3	0.163
Young's Modulus, psi	
70°F	60×10^6
2000°F	55×10^6
Specific Heat, Btu/lb/°F	0.15
Thermal Conductivity, Btu/hr/ft/°F	15
Coefficient of Thermal Expansion, per°F	4.8×10^{-6}
Bend Strength at 2000°F, psi	40,000
Oxidation Resistance at 2500°F, in./hr	0.006

III. PRATT & WHITNEY AIRCRAFT - MECHANICAL TESTS

TIKOTE®-C erosion resistant coating and nickel intermediate layer were applied by Texas Instruments, Inc., to various uncoated specimens supplied by Pratt & Whitney Aircraft to determine the effects of the coating on the mechanical properties of the alloy substrate over a range of temperatures to 900°F. Mechanical tests were conducted by Pratt & Whitney Aircraft in accordance with the requirements of AMMRC Contract DAAG46-71-C-0173. A complete list of the mechanical tests performed is provided in Table III. Also listed in Table III are the limited tests performed by P&WA on TiB_2 coated test specimens prepared by UARL.

TABLE III. LIST OF TESTS PERFORMED BY P&WA UNDER AMMRC CONTRACT DAAG46-71-C-0173

Type	Temperature, °F	Number of Specimens	Specimen Coating
Adhesion-Shear	Room	8	TIKOTE®-C
Adhesion-Tension	Room	4	TIKOTE®-C
Adhesion-Peening	Room	3	TIKOTE®-C
Thermal Shock	400	4	TIKOTE®-C
	900	5	TIKOTE®-C
Stress Corrosion	900	5	Bare
	900	7	TIKOTE®-C
	900	6	Prefatigued TIKOTE®-C
Tensile	Room	2	Bare
	Room	2	Masked
	Room	3	TIKOTE®-C
	900	2	Bare
	900	2	Masked
	900	4	TIKOTE®-C
Creep	900	4	Bare
	900	2	Masked
	900	4	TIKOTE®-C
High-Cycle Fatigue	Room	10	Bare
	Room	6	Masked
	Room	6	TiB_2
	Room	6	TIKOTE®-C
	900	6	Bare
	900	6	Masked
	900	7	TIKOTE®-C
JT8D Blade Fatigue, P/N 571206	Room	7	Bare
	Room	7	TIKOTE®-C Root Masked
	Room	7	TIKOTE®-C
	Room	3	Nickel Plated

TABLE III. LIST OF TESTS PERFORMED BY P&WA UNDER AMMRC CONTRACT DAAG46-71-C-0173 (Continued)			
Type	Temperature, °F	Number of Specimens	Specimen Coating
Erosion Resistance (each condition at 20- and 90-deg angles)	Room	2	Bare
	400	2	Bare
	900	2	Bare
	Room	4	TiB_2
	Room	4	TIKOTE®-C
	400	4	TIKOTE®-C
	900	4	TIKOTE®-C

The test program was divided into two general categories: (1) tests that deal with the properties and integrity of the coating, and (2) tests that measure the effects of the coating on the mechanical properties of the alloy. Some specimens were masked for the purpose of separating the effects of the coating and the effects of the chemical vapor deposition thermal process associated with the application of the coating. Control specimens from the same alloy heat were tested, where applicable, to provide baseline data.

Tests That Deal With Properties of the Coating

Coating Adhesion

The adhesion strength of the TIKOTE-C coating was determined in both shear and tension with the specimens shown in Figure 19. Shear tests were conducted at room temperature by the method described in Appendix III. The average shear strength of eight specimens was 2743 psi over a range of values from 1628 psi to 3995 psi. (See Table IV.) In all cases, failure occurred at the titanium/nickel interface.

Adhesion in tension was determined at room temperature by the method described in Appendix IV. An average of four specimens was 9,360 psi in tension, over a range of values from 7,860 psi to 10,290 psi. (See Table V.) All failures were again located at the titanium/nickel interface.

On the basis of the failure locations, it was determined that the limiting factor, which determines coating adhesion strength, is the integrity of the bond between the nickel plate and the titanium substrate. Microscopic examination showed several voids at this interface.

The effect of a moderate glass bead peen was also used as an indicator of coating adhesion. Specimens were subjected to peening at an intensity of 8-10 N2. This treatment removed part of the coating, as shown in Figure 20. The nickel plate was removed with the TIKOTE-C on all the specimens, thus exposing the bare titanium in the areas where the coating system was removed.

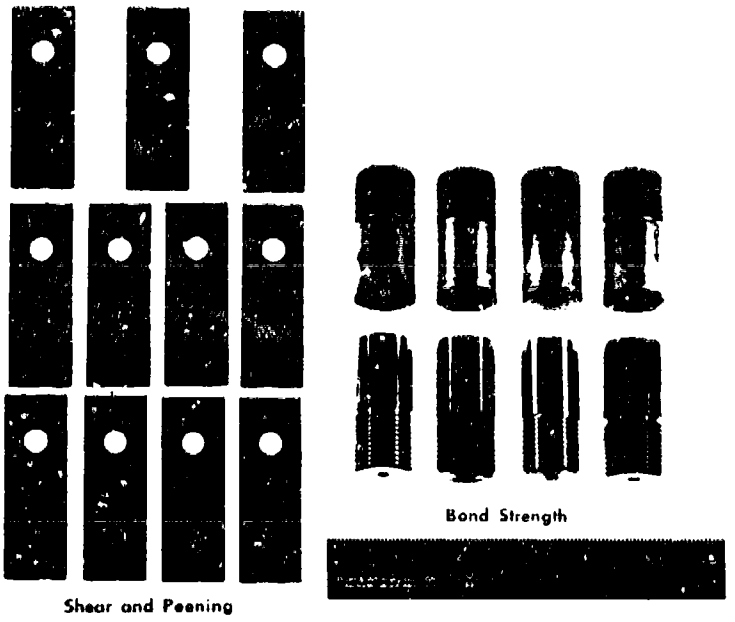

Figure 19. Specimens Used to Evaluate Adhesion Strength. FE 119520

Figure 20. Typical Specimen After Peening Test. FE 122497

TABLE IV. ADHESION IN SHEAR		
Base Material		Ti-6Al-4V Sheet Stock
Temperature		Room Temperature
Adhesive		Nylon Epoxy Bonding Film
Specimen Number	Shear Strength, psi	Failure Location
1	2450	Titanium/Nickel
2	2120	Titanium/Nickel
3	1885	Titanium/Nickel
4	3960	Titanium/Nickel
5	3995	Titanium/Nickel
6	2730	Titanium/Nickel
7	3175	Titanium/Nickel
8	1628	Titanium/Nickel
Average	2743	

TABLE V. ADHESION IN TENSION		
Base Material		Ti-6Al-4V Bar Stock
Temperature		Room Temperature
Adhesive		Scotchweld Epoxy
Specimen Number	Tensile Strength, psi	Failure Location
1	10,110	Titanium/Nickel
2	10,290	Titanium/Nickel
3	9,180	Titanium/Nickel
4	7,860	Titanium/Nickel
Average	9,360	

Thermal Shock Cycling

In devising a test to evaluate the coating's resistance to thermal shock, it was decided to employ the tubular-shaped specimens shown in Figure 21 because of: (1) ease of obtaining a continuous coated surface around the tube OD, (2) adaptability to induction heating for fast temperature response, and (3) ease of cooling by passing coolant through the tube ID. The test specimens were 0.500-in. OD by 0.031-in. wall thickness by 6-in. long tubes of Ti-3Al-2.5V alloy coated with TIKOTE-C. Alloy Ti-3Al-2.5V was used for the tubular thermal shock specimens because Ti-6Al-4V was not available in tube form.

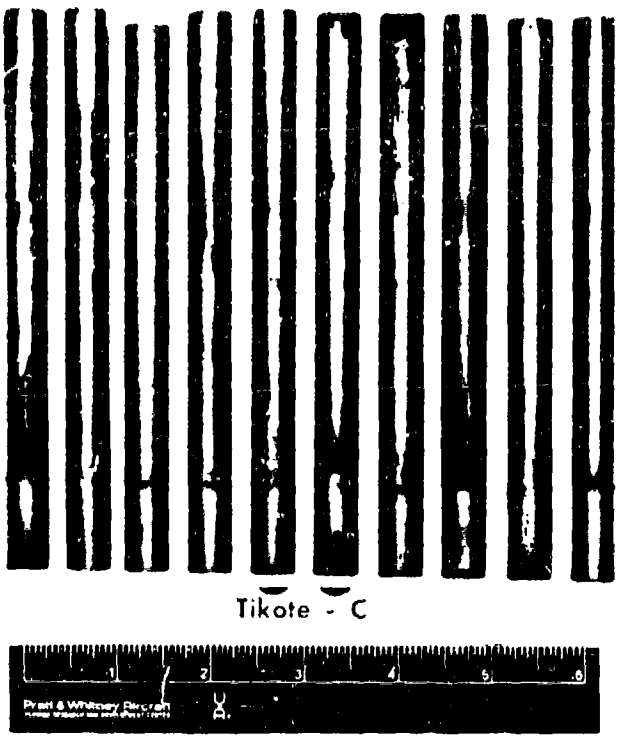

Figure 21. Thermal Shock Tubular Specimens. FE 120485

Each tube was mounted with one end unrestricted to allow free thermal expansion. Thermal cycling was accomplished by alternately induction heating the surface and forcing cooling air through the inside of the tube. The test setup is illustrated schematically in Figure 22. Cyclic rate was approximately 3 cycles per minute (8-sec heating and 13-sec cooling) for all tests. Each tube was thermally cycled for 100 cycles, with test interruptions every 10 cycles for visual inspection of the coating. Five tubes were cycled from room temperature to 900°F and four were cycled from room temperature to 400°F.

Temperature for the 900°F tests was monitored via a radiation pyrometer and, for the 400°F tests, an internal (to the tube) thermocouple was employed. Thermal cycling from room temperature to 400°F and from room temperature to 900°F had no adverse effect on the TIKOTE-C coating bond. The only effect was a change in color to deep blue of those specimens heated to 900°F.

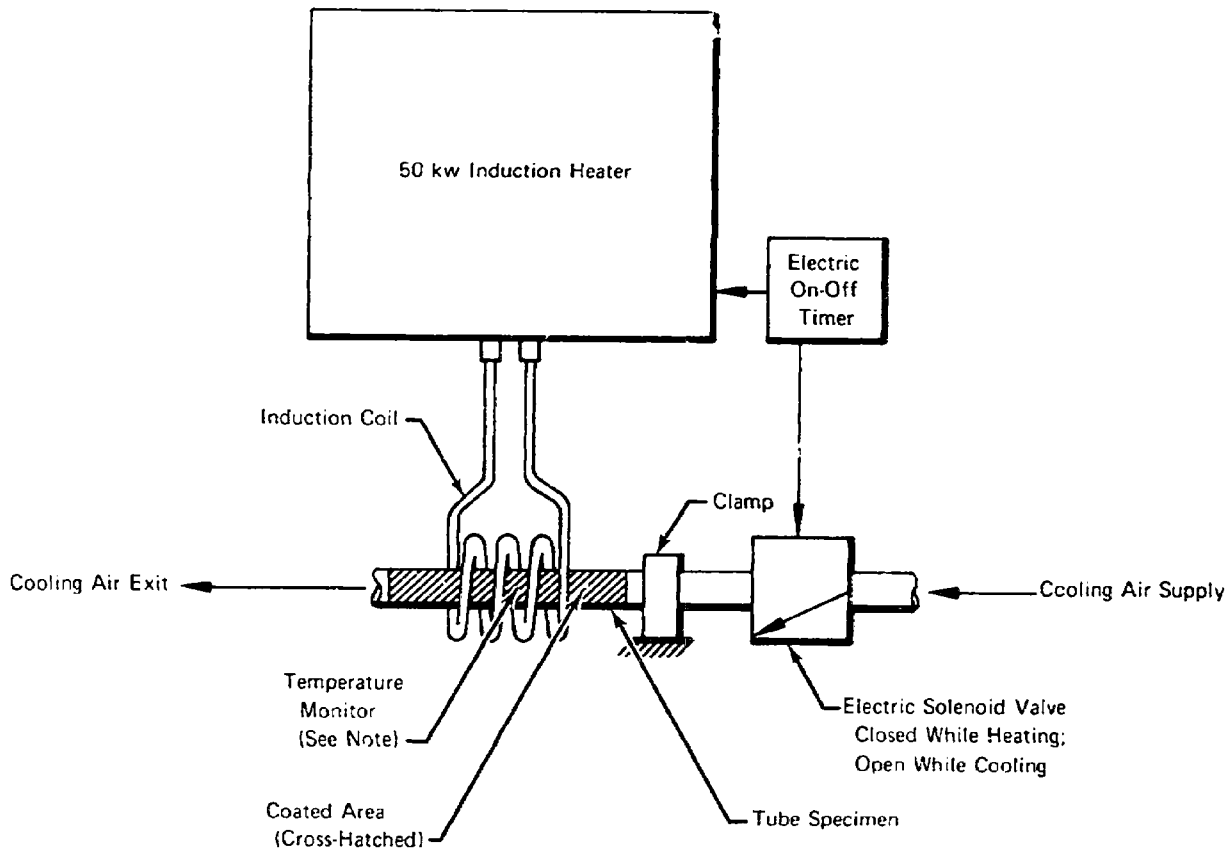

Note: Temperature monitored by noncontract radiation pyrometer for 900°F tests and by internal (to tube) for 400°F tests

Figure 22. Test Setup Schematic for Repeated Thermal Shock Testing.

FD 65121

It should be noted that Texas Instruments, Inc., was unable to nickel plate the tubular Ti-3Al-2.5V thermal shock specimens using their usual techniques and, also, neither could they plate pure titanium. The specimens were plated by Pratt & Whitney Aircraft Experimental Shops, with a 0.0001 to 0.0002 in. of electroless nickel per PWA™ 36 without heat treatment. These specimens were subsequently coated with TIKOTE-C by Texas Instruments, Inc., without additional electrolytic nickel plating. PWA 36 is a new proprietary acid bath phosphorous nickel plating process with a copper strike that was not available at the beginning of the program.

Hot Salt Stress Corrosion

Hot salt stress corrosion susceptibility was evaluated by the P&WA™ method described in Appendix V. Tests were conducted at 900°F and 50-ksi static stress with salt contamination from a 3 percent sodium chloride solution using the specimens shown in Figure 23. Three types of specimens were tested: (1) uncoated Ti-6Al-4V specimens (to serve as a control); (2) specimens coated with TIKOTE-C; and (3) specimens coated with TIKOTE-C, which were subsequently cracked (prefatigued) by flexing the specimens. The specimens were examined after a 100-hr period, and all had failed, including the control specimens. The TIKOTE-C coating and nickel plating interlayer offered no protection from hot salt stress corrosion in either condition.

Figure 23. Hot Salt Stress Corrosion Specimens. FE 119523

Other P&WA hot salt stress corrosion tests with just nickel-plated titanium specimens have gone over 150 hr with no failures. This suggests that cracks in the TIKOTE-C coating may propagate through the nickel plating interlayer into the titanium.

Erosion Resistance

Erosion resistance of TIKOTE-C (titanium carbonitride) applied to nickel-plated Ti-6Al-4V alloy was evaluated at 20- and 90-deg abrasion impingement angles at room temperature, 400 and 900°F using the specimens shown in Figure 24. A second coating, titanium diboride, TiB_2, developed by the United Aircraft Research Laboratory, was included in the room temperature erosion testing portion of the overall program as a backup coating. Both coatings were significantly more erosion resistant than uncoated Ti-6Al-4V alloy at all test conditions.

Erosion testing was performed with an SS White Airbrasive Unit (Figure 25 using 27μ aluminum oxide as the abrasive. The abrasive powder was stored in a glass vessel containing a dessicant and kept under vacuum until needed. This procedure ensured a minimum amount of moisture in the powder and more control over the apparatus. Abrasive flowrate was calculated at 113 mg/sec at an air pressure of 60 psig. This rate represents the average of seven runs. The apparatus was calibrated on a standard specimen after each test to ensure uniform and constant abrasive action throughout the test program. Specimen temperature was monitored by means of a thermocouple attached to the back of the test specimen. A Honeywell Temperature Controller was used to maintain temperature. Specimens were allowed to equilibrate for 10 min at the desired temperature prior to testing. During the test, the onrushing air carrying the abrasive caused a drop in specimen temperature. Preheating the tube, through which the abrasive flowed, limited by the rubber material used for carrying the air stream, still resulted in a decrease in temperature of the test specimen.

Each test run was monitored by an operator, who constantly observed the test. For coated specimens, the test was completed at the first sign of "sparks," which denoted penetration of the coating into the basic metal. The time needed to reach this point was recorded. Neither TIKOTE-C nor titanium diboride coatings sparked while being eroded. This procedure was then repeated. Uncoated specimens were eroded for specified times of 9, 18, 36, and 54 sec. All tested specimens were metallographically examined through eroded areas.

The times to penetrate the coatings into the basic metal are listed in Table VI. Metallographic examination of eroded specimens yielded coating thickness measurements that are also included in Table VI. These data are for the total coating system, i.e., nickel-plate diffused into the titanium plus nickel plate plus coating. The combination of these data yielded a coating erosion rate on time to penetrate into the basic metal per coating mil also listed in Table VI.

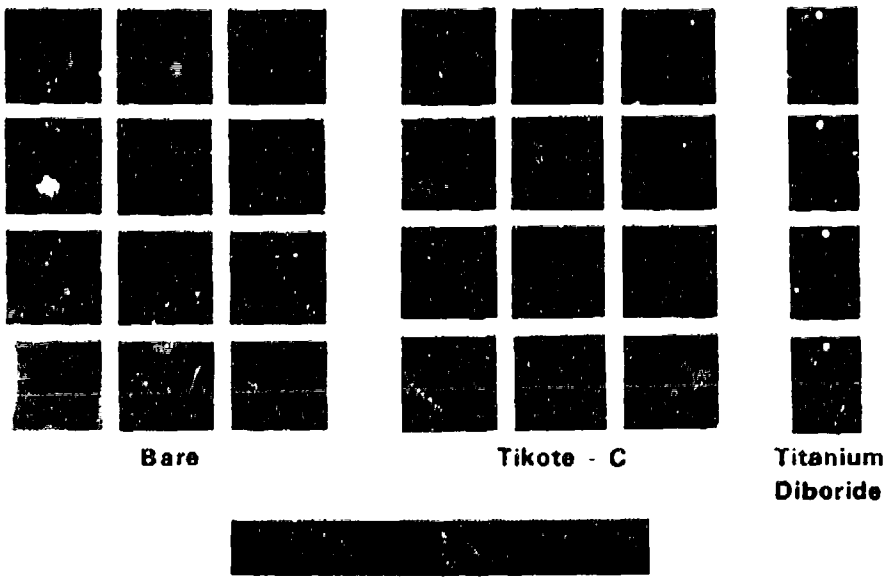

Figure 24. Specimens Used to Evaluate Erosion Resistance FC 27307

Data for the TIKOTE-C coating system indicated that, for 20- and 90-deg impingement angles, as temperature increased, erosion resistance increased, reached a maximum, and decreased. Irrespective of temperature, both TiB_2 and TIKOTE-C coatings were more erosion resistant at the 20-deg angle. The TiB_2 system had more than twice the erosion resistance of TIKOTE-C at 20-deg and half the erosion resistance at the 90-deg impingement angle. A summary of coated and uncoated test results, showing the degree of increased erosion resistance relative to uncoated Ti-6Al-4V, is presented in Table VII. Both coatings provided substantial improvement in erosion resistance, compared to the uncoated Ti-6Al-4V alloy, i.e., > 125 x improvement at 20 deg and > 10 x at 90 deg.

Metallographic examination of coated specimens revealed the presence of three coating layers: (1) nickel plate, which diffused into the titanium, (2) nickel plate, and (3) TIKOTE-C or TiB_2. The thickness of diffused nickel and nickel-plated regions was 0.1- to 0.25-mil per layer on TIKOTE-C coated specimens. Thickness of the TIKOTE-C was 0.5 - 0.9 mil. Specimens for TiB_2 coating were supplied to UARL in the nickel-plated condition. After applying the TiB_2 coating, it was noted that the nickel plate spalled from the Ti-6Al-4V substrate. These specimens were stripped and electrolytic nickel plated by P&WA. No spalling occurred after the subsequent application of TiB_2. Examination of these specimens indicated a 0.2- to 0.25-mil diffused nickel layer, 0.5- to 0.7-mil nickel plate, and 0.25- to 0.6-mil of TiB_2. The TiB_2 coated specimen, tested at the 90-deg impingement angle, had 0.5-mil of nickel plate, which amounted to 50% of the total coating, and only 0.25-mil of actual TiB_2. This thickness of TiB_2 is not sufficient for maximum erosion resistance. If 0.6-mil of TiB_2 had been applied, as on the 20-deg test specimen, then the erosion rate of the TiB_2 system might have been comparable to that of TIKOTE-C.

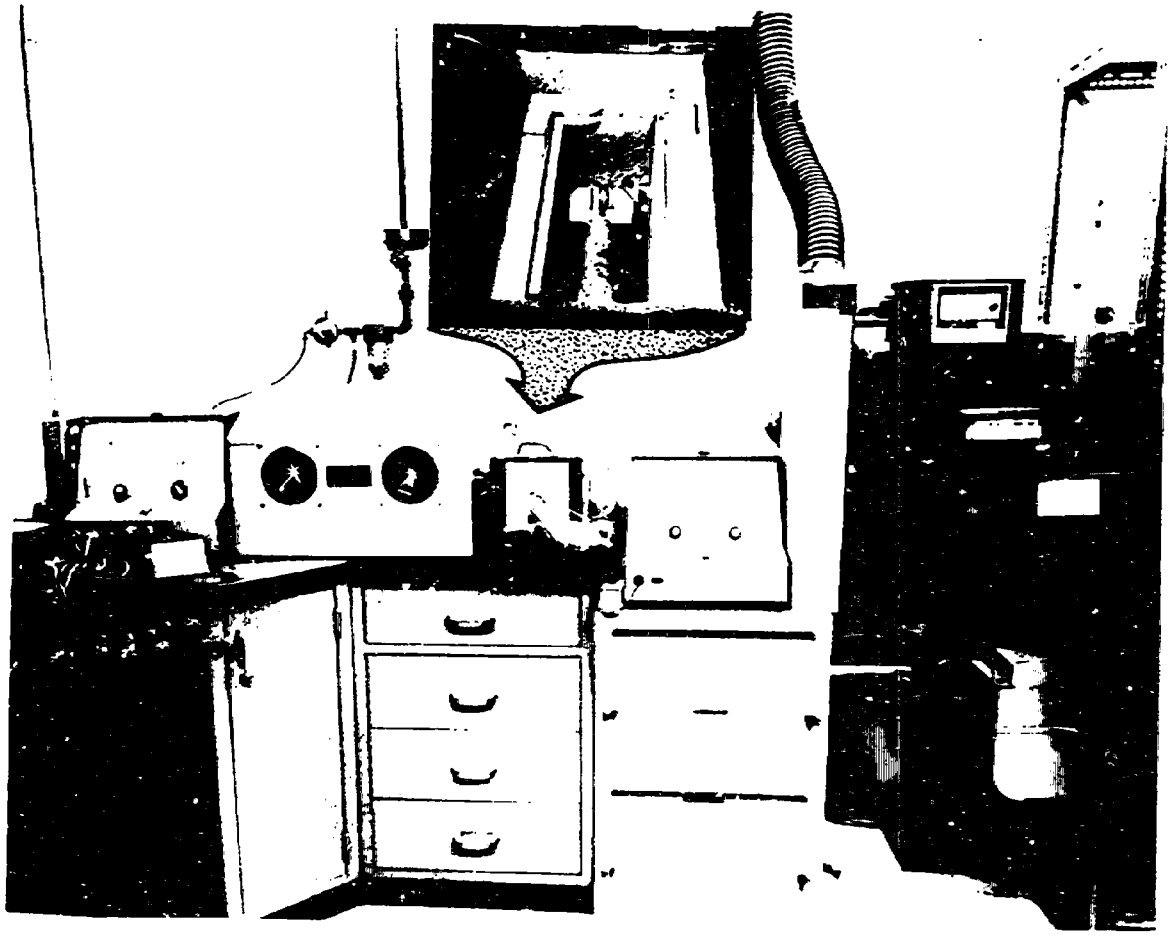

Figure 25. SS White Abrasive Unit, Temperature Controls and Readout.

FD 65124

TABLE VI. EROSION DATA FOR TWO COATING SYSTEMS ON Ti-6Al-4V ALLOY

	20 deg			90 deg		
	Room Temperature	400°F	900°F	Room Temperature	400°F	900°F
Diffused Ni+Ni Plate + TiB_2						
Time to penetrate, sec	1808, 2238	-	-	43, 45	-	-
Coating thickness, 0.001 in.	1.4 1445[1]	-	-	1.0 44	-	-
Erosion rate, sec/0.001 in. of coating	1291, 1599	-	-	43, 45	-	-
Diffused Ni+Ni Plate + TIKOTE®-C						
Time to penetrate, sec	718, 918	1885, 2215	951, 1775	50, 75	60, 207	36, 57
Coating thickness, 0.001 in.	1.2 682	1.2 1708	1.0 1363	0.7 89	0.7 191	1.1 43
Erosion rate, sec/0.001 in. of coating	598, 765	1570, 1846	951, 1775	71, 107	86, 296	33, 52
Uncoated Ti-6Al-4V						
Erosion rate, sec/0.001 in.	5.0	5.4	9.0	3.2	6.3	4.5

[1] The average of the two test runs.

TABLE VII. EROSION RESISTANCE OF COATINGS ON Ti-6Al-4V RELATIVE TO UNCOATED Ti-6Al-4V						
	20 deg			90 Deg		
Coating System	Room Temperature	400°F	900°F	Room Temperature	400°F	900°F
Diffused Ni-Ni Plate + TiB_2	289x	-	-	11x	-	-
Diffused Ni-Ni Plate TIKOTE®-C	136x	316x	151x	28x	30x	9.6x

Tests That Measure the Effects of the Coating on Mechanical Properties of the Alloy

Tensile Tests

Tensile tests were conducted at room temperature and at 900°F on uncoated specimens, on specimens that were masked in the gage section and then processed, and on specimens nickel-plated and coated with TIKOTE-C. A photograph of the tensile test specimens is presented in Figure 26.

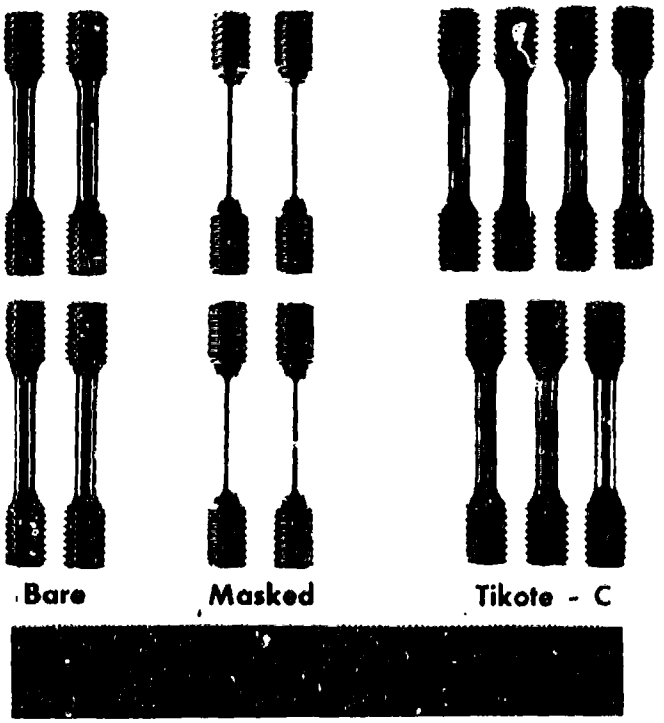

Figure 26. Tensile Test Specimens. FE 119521

Room temperature tensile properties are shown in Table VIII. It is evident that neither the coating process nor the coating itself has any significant effect on room temperature tensile properties.

Elevated temperature tensile properties are shown in Table IX. Again, there is little difference among the three types of specimens, although the effect is slightly more pronounced at 900°F than at room temperature; approximately a 6% loss of tensile strength occurred with the coated specimens.

TABLE VIII. ROOM TEMPERATURE TENSILE PROPERTIES

Base Material				Ti-6Al-4V Bar Stock	
Temperature				Room Temperature	
Specimen Number	Specimen Condition	0.2% Offset Yield Strength, psi	Tensile Strength, psi	Elongation, %	Reduction of Area, %
1	Bare	149,700	149,700	16.0	55.1
2	Bare	151,500	151,500	17.5	52.6
3	Masked	144,000	144,000	16.0	49.9
4	Masked	146,000	146,000	17.0	49.1
5	Coated	148,700	150,300	16.0	45.6
6	Coated	150,100	150,300	16.0	51.0
7	Coated	149,400	150,100	18.0	51.1

TABLE IX. 900°F TENSILE PROPERTIES

Base Material				Ti-6Al-4V Bar Stock	
Temperature, °F				900	
Specimen Number	Specimen Condition	0.2% Offset Yield Strength, psi	Tensile Strength, psi	Elongation, %	Reduction of Area, %
1	Bare	81,400	91,700	26.5	76.0
2	Bare	81,500	92,400	26.0	75.6
3	Masked	79,400	89,900	25.0	70.8
4	Masked	79,000	90,300	26.5	71.8
5	Coated	75,000	87,600	27.5	72.7
6	Coated	76,000	85,500	25.5	73.5
7	Coated	76,400	85,000	28.0	72.6
8	Coated	75,000	86,000	29.5	75.4

Creep Properties

The specimens used to evaluate the effect of the coating on creep properties of titanium are shown in Figure 27. Experience with the creep properties of the Ti-6Al-4V alloy at 900°F is limited. Therefore, experimentation was necessary to establish the appropriate stress level for test purposes. Specimens run at 35 and 25 ksi creeped to 1.0% in 5.5 and 43.3 hr, respectively. This was considered excessive and the stress level was lowered to 15 ksi, where the remainder of the specimens were run.

The masked and coated specimens performed similarly, both running somewhat over 100 hr to 1.0% creep. Comparison with the uncoated condition indicates that the bare specimens reached 1% creep somewhat sooner (Table X).

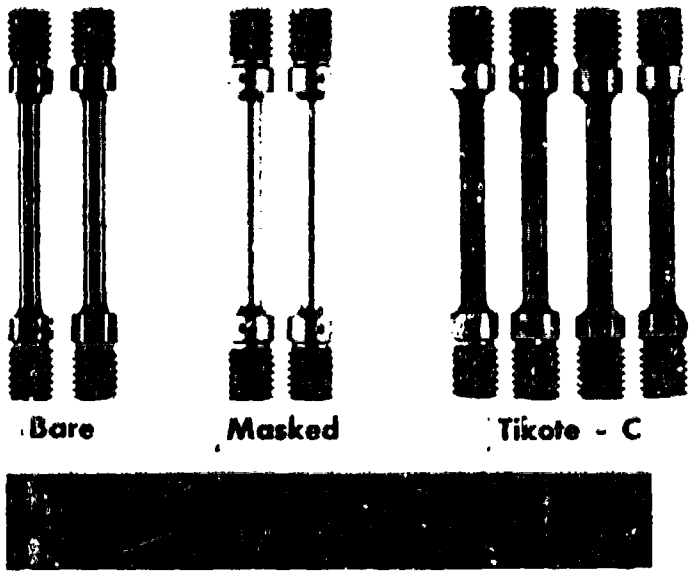

Figure 27. Creep Specimens. FE 119522

TABLE X. 900°F CREEP PROPERTIES

Base Material			Ti-6Al-4V Bar Stock
Specimen Number	Specimen Condition	Stress Level	Hours to 1.0% Creep
1	Bare	15,000	54.4
2	Masked	15,000	107.9
3	Masked	15,000	113.1
4	Coated	15,000	81.2
5	Coated	15,000	110.5
6	Coated	15,000	128.0
7	Bare	35,000	5.5
8	Coated	25,000	43.3
9	Bare	15,000	57.0
10	Bare	15,000	70.5

High-Cycle Fatigue

Rotating beam fatigue tests were conducted at room temperature on the Ti-6Al-4V bar stock specimens shown in Figure 28, that had been masked, on specimens nickel-plated and coated with TIKOTE-C, and on specimens nickel-plated and coated with TiB_2. Elevated temperature tests were conducted on masked and TIKOTE-C specimens only. In both cases, uncoated specimens from the same alloy heat provided baseline data. Conditions of the tests were room temperature, 900°F and at a cyclic stress reversal frequency of 100 Hz.

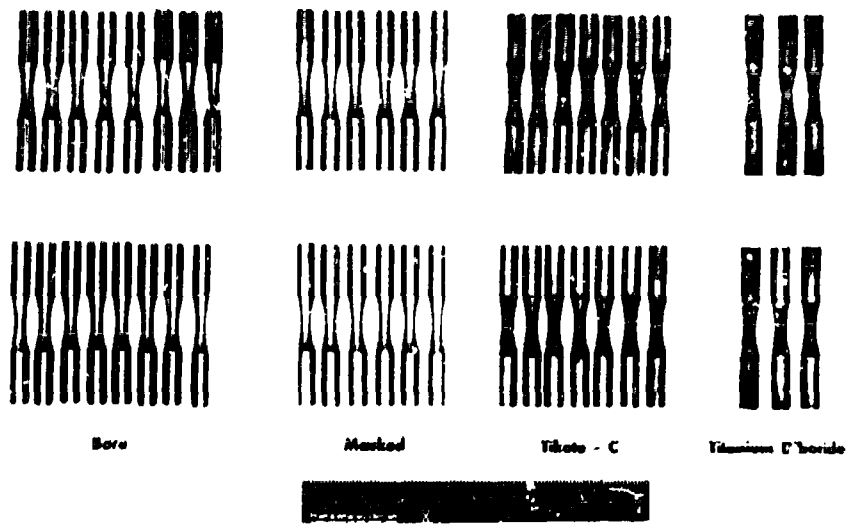

Figure 28. Rotating Beam Fatigue Test Specimens FE 120407

Reverse bending fatigue results at 10^7 cycles indicated the following:

1. TIKOTE-C coating reduced the fatigue life of Ti-6Al-4V approximately 63% (67.5 to 25.0 ksi) at room temperature and approximately 58% (47.5 to 20.0 ksi) at 900°F.

2. The application of TiB_2 coating to Ti-6Al-4V also reduced the fatigue life of the base material approximately 63% (67.5 to 25.0 ksi) at room temperature.

3. The fatigue life of masked specimens was essentially unchanged (67.5 to 70 ksi) at room temperature, and increased 26% (47.4 to 60.0 ksi) at 900°F.

High-cycle fatigue results are listed in Tables XI and XII and are plotted in Figures 29 and 30 for room temperature and 900°F conditions, respectively.

Note: Masked specimens were uncoated but subjected to the TIKOTE-C process environment.

TABLE XI. ROOM TEMPERATURE ROTATING BEAM FATIGUE RESULTS

Specimen Number	Surface Condition	Test Stress, ksi	Test Cycles	Results
34	As-received, uncoated	80	1.0×10^6	Failed
35	As-received, uncoated	75	3.9×10^4	Failed
36	As-received, uncoated	70	1.8×10^5	Failed
37	As-received, uncoated	60	1.0×10^7	Did not fail
38	As-received, uncoated	60	1.0×10^7	Did not fail
39	As-received, uncoated	85	3.3×10^4	Failed
40	As-received, uncoated	90	4.7×10^4	Failed
41	As-received, uncoated	65	1.0×10^7	Did not fail
42	As-received, uncoated	67.5	1.0×10^7	Did not fail
43	As-received, uncoated	67.5	1.0×10^7	Did not fail
1	Masked (subjected to TIKOTE® -C process)	70	1.0×10^7	Did not fail
2	Masked (subjected to TIKOTE® -C process)	72.5	1.2×10^5	Failed
3	Masked (subjected to TIKOTE® -C process)	70	1.0×10^7	Did not fail
4	Masked (subjected to TIKOTE® -C process)	75	1.0×10^7	Did not fail
5	Masked (subjected to TIKOTE® -C process)	80	1.2×10^5	Failed
6	Masked (subjected to TIKOTE® -C process)	90	3.5×10^4	Failed
13	TiB_2 coated	75	2.4×10^4	Failed
14	TiB_2 coated	65	3.9×10^4	Failed
16	TiB_2 coated	55	1.2×10^5	Failed
17	TiB_2 coated	45	7.1×10^5	Failed
18	TiB_2 coated	35	1.7×10^6	Failed
19	TiB_2 coated	25	1.0×10^7	Did not fail
20	TIKOTE® -C coated	65	2.0×10^4	Failed
21	TIKOTE® -C coated	55	2.4×10^4	Failed
22	TIKOTE® -C coated	45	2.1×10^5	Failed

TABLE XI. ROOM TEMPERATURE ROTATING BEAM FATIGUE RESULTS (Continued)				
Specimen Number	Surface Condition	Test Stress, ksi	Test Cycles	Results
23	TIKOTE®-C coated	35	1.9×10^5	Failed
24	TIKOTE®-C coated	25	1.0×10^7	Did not fail
25	TIKOTE®-C coated	35	2.4×10^5	Failed
26	TIKOTE®-C coated	30	1.0×10^7	Did not fail

TABLE XII. ROTATING BEAM FATIGUE RESULTS AT 900°F				
Specimen Number	Surface Condition	Test Stress, ksi	Test Cycles	Results
44	As-received, uncoated	60	2.9×10^4	Failed
45	As-received, uncoated	50	6.1×10^4	Failed
46	As-received, uncoated	40	1.0×10^7	Did not fail
47	As-received, uncoated	45	1.0×10^7	Did not fail
48	As-received, uncoated	47.5	1.0×10^7	Did not fail
49	As-received, uncoated	47.5	1.0×10^7	Did not fail
7	Masked (subjected to TIKOTE®-C process)	75	1.1×10^4	Failed
8	Masked (subjected to TIKOTE®-C process)	60	1.0×10^7	Did not fail
9	Masked (subjected to TIKOTE®-C process)	70	2.6×10^4	Failed
10	Masked (subjected to TIKOTE®-C process)	65	1.3×10^6	Failed
11	Masked (subjected to TIKOTE®-C process)	60	3.7×10^6	Failed
12	Masked (subjected to TIKOTE®-C process)	55	1.0×10^7	Did not fail
27	TIKOTE®-C coated	45	3.1×10^4	Failed
28	TIKOTE®-C coated	25	1.6×10^5	Failed
29	TIKOTE®-C coated	15	1.0×10^7	Did not fail
30	TIKOTE®-C coated	20	1.0×10^7	Did not fail
31	TIKOTE®-C coated	20	1.0×10^7	Did not fail
32	TIKOTE®-C coated	25	1.0×10^7	Did not fail
33	TIKOTE®-C coated	35	4.6×10^4	Failed

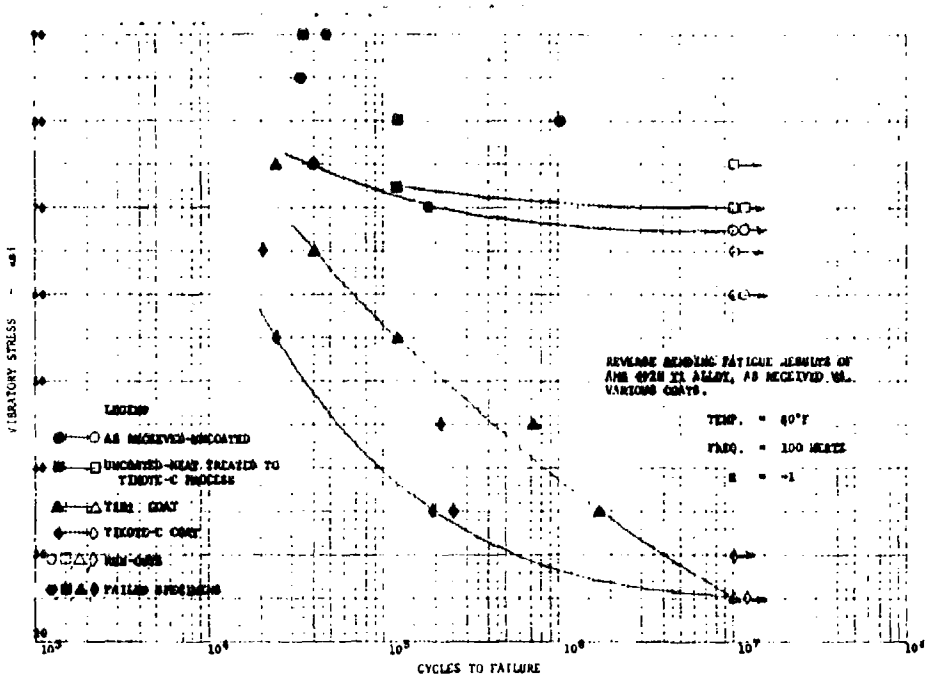

Figure 29. Reverse-Bending, High-Cycle Fatigue Results at Room Temperature. DF 92813

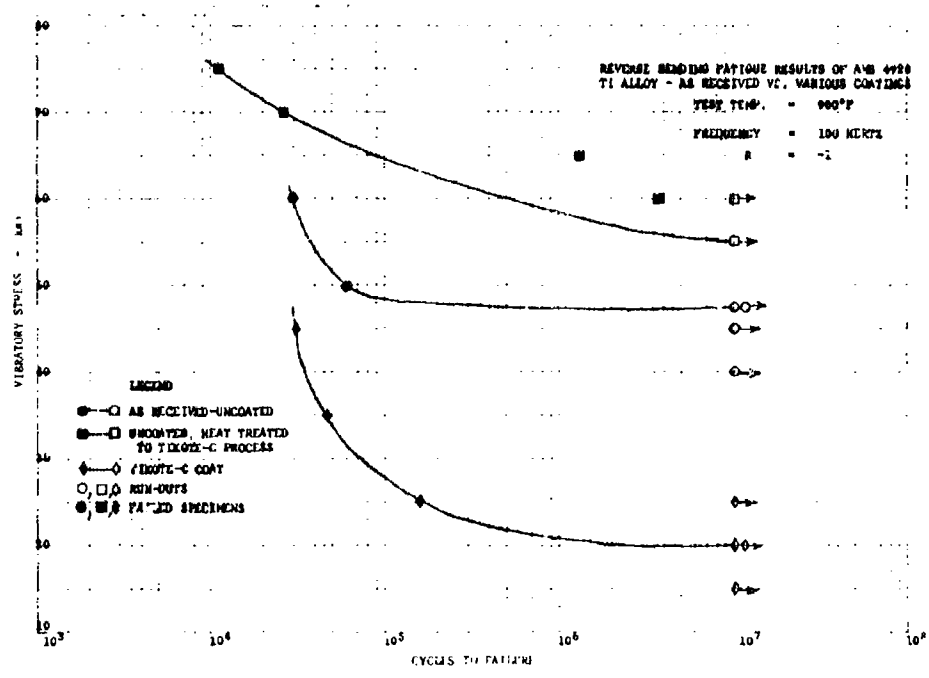

Figure 30. Reverse-Bending, High-Cycle Fatigue Results at 900°F. DF 92814

Blade Fatigue Testing

Room temperature first-bending mode, high-cycle fatigue tests were conducted to determine the effects of applying TIKOTE-C to airfoil hardware. JT8D 6th-stage compressor blades (P/N 571206, Ti-6Al-4V) were selected for the tests due to their availability. Four conditions tested were: (1) uncoated blades, to establish a baseline, (2) blades with nickel plate covering 100% of airfoil, (3) blades nickel plated with TIKOTE-C overlay covering 100% of airfoil, and (4) blades nickel plated with TIKOTE-C overlay covering 50% of airfoil (midspan to tip). Typical JT8D 6th-stage compressor blade test specimens with each type of surface treatment are shown in Figure 31.

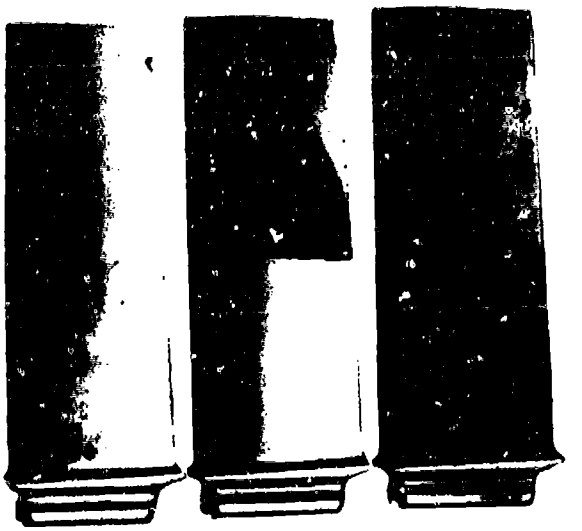

(A) (B) (C)

FAL 25915

(A) Nickel Plate Covering 100% of Airfoil

(B) Nickel Plate With TIKOTE®-C Overlay Covering 50% of Airfoil From Midspan to Tip (Dark Area)

(C) Nickel Plate With 100% TIKOTE®-C Overlay 100% of Airfoil

Figure 31. Typical JT8D 6th-Stage Axial Compressor Blades Showing the Three Different Types of Surface Treatments. FD 65128

The location and orientation of calibration strain gages were determined from stresscoat patterns and/or failure locations resulting from the first bending mode of vibration (Figure 32). Strain gages were applied to three blades of each configuration and individual average dynamic stress vs double amplitude curves established for each. Each blade configuration was tested according to its established calibration curve. Fatigue tests were conducted on the blades at room temperature in the first bending mode of vibration. Test results are tabulated in Table XII and the established stress vs cycles-to-failure curve (S/N) for 10^7 cycles for each type surface treatment is presented in Figure 33.

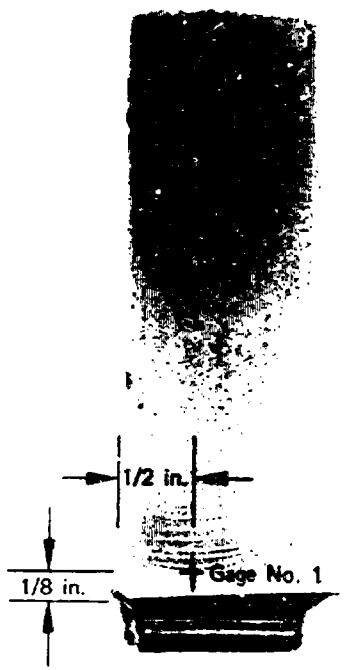

FAL 25615

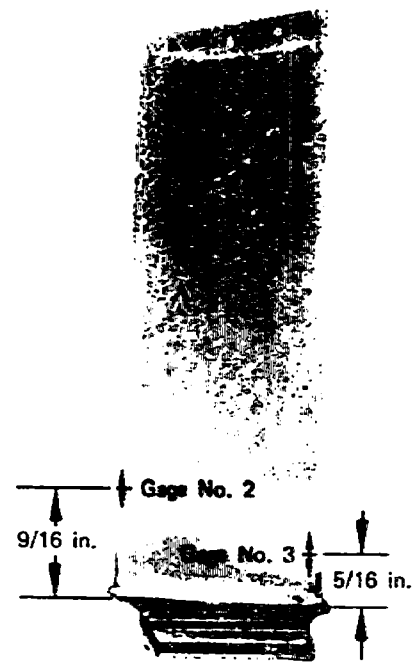

FAL 25616

Figure 32. Typical Stresscoat Patterns and Strain Gage Locations in First Bending Mode of Vibration. FD 65129

TABLE XIII. FATIGUE DATA - JT8D 6TH-STAGE AXIAL COMPRESSOR BLADE, P/N 571206, TESTED AT ROOM TEMPERATURE IN FIRST BENDING MODE

S/N[1]	Airfoil Stress, psi [2]	Cycles	Remarks
1B	66,500[3]	10×10^6	Did not fail
3B	66,500[3]	10×10^6	Did not fail
4B	62,500[3]	10×10^6	Did not fail
5B	85,000	5.57×10^6	Failed at the MRT
6B	75,000	0.98×10^6	Failed 15/32 in. from platform on TE
2B	80,000	0.024×10^6	Failed 9/16 in. from platform on TE
7B	54,000[3]	10×10^6	Did not fail
1C	82,500	0.0012×10^6	Failed 5/16 in. from platform on LE
4C	72,500	0.0024×10^6	Failed 5/16 in. from platform on LE
7C	60,000	0.0048×10^6	Failed 5/32 in. from platform on LE
6C	33,500	0.72×10^6	Failed 15/32 in. from platform on TE
3C	27,800	0.12×10^6	Failed 5/16 in. from platform on TE
5C	15,200[3]	10×10^6	Did not fail
2C	21,500[3]	10×10^6	Did not fail
1P	75,000	0.046×10^6	Failed at the MRT
2P	45,500	0.228×10^6	Failed in a blended nick on the TE - not used for data
3P	65,000[4]	10×10^6	Did not fail

[1] S/N denotes surface treatment:

- B - Untreated
- C - Nickel plated with TIKOTE®-C overlay covering 100% of airfoil
- P - Nickel plated over 100% of airfoil
- M - Nickel plated with TIKOTE®-C overlay covering 50% of airfoil from midspan to tip (Figure 31)

[2] Stress measured at failure location

[3] Measured at TE (Gage No. 2, Figure 32)

[4] Measured at the MRT (Gage No. 1, Figure 32)

[5] Measured at TE (Gage No. 5, Figure 35)

TABLE XIII. FATIGUE DATA - JT8D 6TH-STAGE AXIAL COMPRESSOR BLADE, P/N 571206, TESTED AT ROOM TEMPERATURE IN FIRST BENDING MODE (Continued)

S/N[1]	Airfoil Stress, psi [2]	Cycles	Remarks
1M	64,000	0.068×10^6	Failed 1-5/16 in. from platform through drip on TE
2M	56,500[3]	10×10^6	Did not fail
3M	71,500	0.19×10^6	Failed 7/16 in. from platform on TE
4M	43,400	0.116×10^6	Failed 1-5/16 in. from platform through drip on TE
5M	36,900	0.38×10^6	Failed 1-15/32 in. from platform on TE
6M	67,700	2.3×10^6	Failed 1/4 in. from platform on TE
7M	34,800	7.4×10^6	Failed 1-3/8 in. from platform on TE
2M	32,600[5]	10×10^6	Did not fail

[1] S/N denotes surface treatment:

- B - Untreated
- C - Nickel plated with TIKOTE® -C overlay covering 100% of airfoil
- P - Nickel plated over 100% of airfoil
- M - Nickel plated with TIKOTE® -C overlay covering 50% of airfoil from midspan to tip (Figure 31)

[2] Stress measured at failure location

[3] Measured at TE (Gage No. 2 Figure 32)

[4] Measured at the MRT (Gage No. 1, Figure 32)

[5] Measured at TE (Gage No. 5, Figure 35)

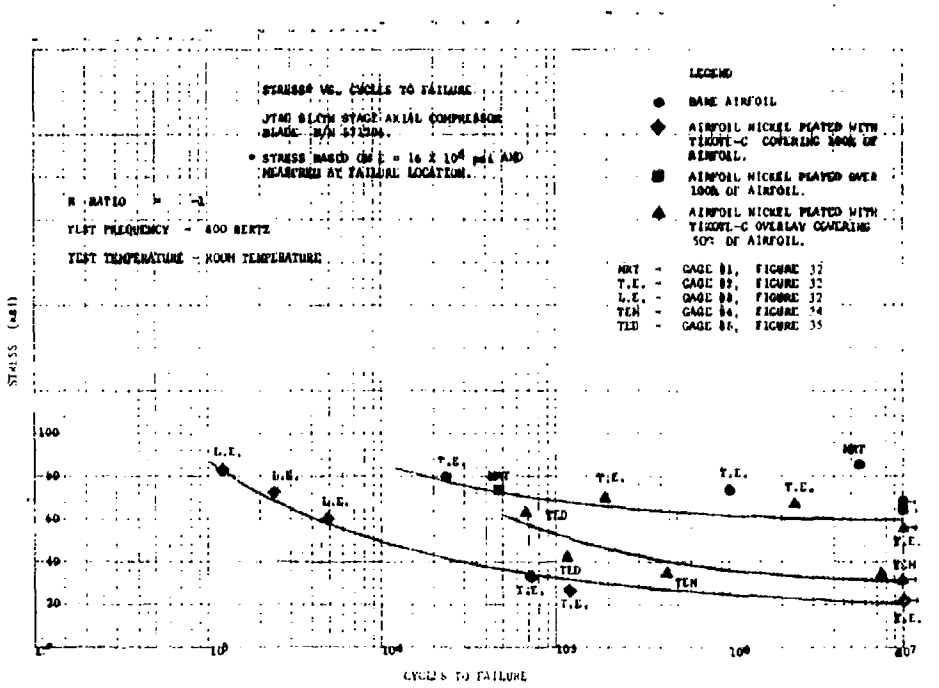

Figure 33. JT8D 6th-Stage Blade Stress vs Cycles to Failure. DF 92815

The application of TIKOTE-C to the masked blades resulted in variations of the failure locations. Figure 34 shows the failure location close to the masking line (1-3/8 in. from the platform on the TE). Figure 35 shows the failure location resulting from an overflow of TIKOTE-C on the untreated portion of the blade (1-5/16 in. from the platform on the TE). A typical failure location of a masked blade (7/16 in. from the platform on the TE) is shown in Figure 36. Masked blades, which failed on the concave TE close to the platform in the masked 50% of the airfoil span, were considered as untreated blades in establishing the S/N curve for bare blades.

The room temperature first bending mode airfoil fatigue strength of the bare untreated JT8D 6th-stage Ti-6Al-4V compressor blade is 60,000 psi at 10^7 cycles. The fatigue strength of blades with nickel plating covering 100% of the airfoil is approximately equal to the untreated blade. Apparently the thin 0.25-mil nickel plate has no effect on the fatigue strength of the blades.

The application of nickel plating and TIKOTE-C resulted in a significant degradation of the fatigue strength established for the untreated airfoils. Those nickel plated and coated with TIKOTE-C covering 100% of the airfoil were degraded 62.5% to 21,500 psi at 10^7 cycles, and those with masked blade roots and nickel plated and coated with TIKOTE-C covering 50% of the airfoil were degraded as much as 39.7% to 36,200 psi at 10^7 cycles.

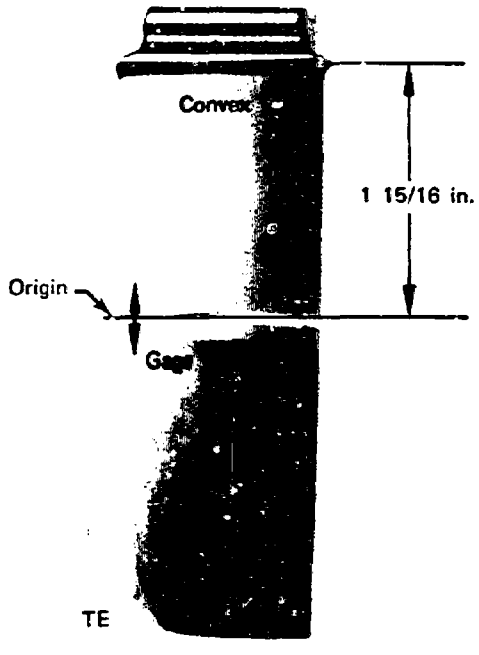

FAL 25814

FAL 25815

Figure 34. Masked JT8D Blade Showing Location of Failure Origin at Edge of TIKOTE®-C.

FD 65130

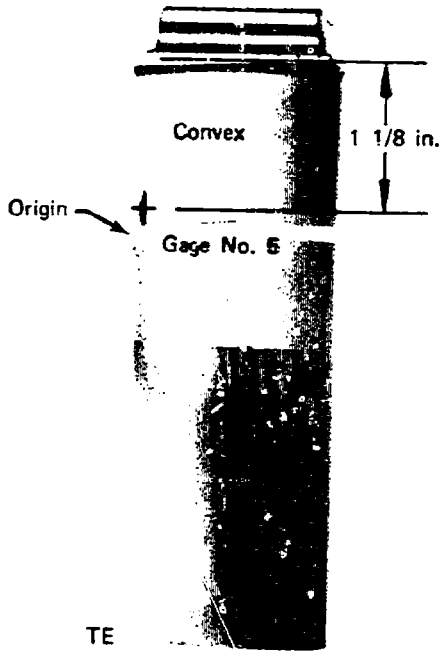

FAL 25816

FAL 25817

Figure 35. J T8D Blade Showing Location of Failure Resulting From TIKOTE®-C Overflow Onto the Masked Portion of the Airfoil.

FD 65131

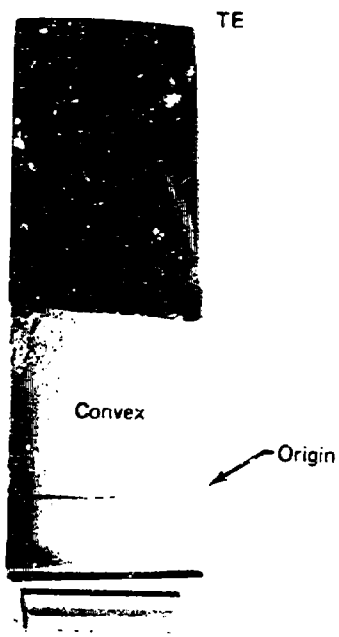

FAL 26007

FAL 26008

Figure 36. Typical Failure in the Uncoated Region of JT8D Masked Blades.

FD 65132

Degradation of the titanium substrate fatigue strength is a result of: (1) fatigue cracking originating in the highly adherent TIKOTE-C coating, which apparently propagates into the base material through the nickel plating in fully coated blades, and (2) grain structure changes in the Ti-6Al-4V base material probably resulting from the accidental high temperatures experienced during preparation of some of the masked blades.

Test results show that TIKOTE-C overlay coating, as applied to the test specimens, should not be used on Ti-6Al-4V airfoils in areas where the reverse bending stress will exceed 21,500 psi.

Metallographic Examination

In addition to the mechanical tests, photomicrographic examinations of two JT8D blades and one PT6 centrifugal impeller were performed.

Sections from the inducer and radial regions of a PT6 A-27 centrifugal impeller (Ti-6Al-4V) were mounted, polished, etched, and examined for coating uniformity and microstructure. Three significant observations were made:

1. Voids were observed between the base metal and the nickel plate. These voids are evident in Figures 26A and B. As noted previously, the adhesion of the coating does not seem to be adversely affected by their presence. This phenomenon was noted in both areas of the impeller and is not localized.

2. A change in base metal structure was observed at the tip of the impeller blades, adjacent to the nickel plate. This was interpreted as a titanium-depleted zone and is attributed to the diffusion of nickel into the substrate. This feature was noted only on the tips of the blade. (See Figure 26C.)

3. The coating thickness varied from 0.0024 in. at the very tip of the blade to 0.0008 to 0.0012 in. over the remainder of the surface. This was true of both sections examined. The nickel plate was also found to be heavier at the tip, and this may be the reason why it was the only area where the effects of nickel diffusion were noted.

Two JT8D 6th-stage axial compressor blades (P/N 571206) were sectioned and examined. One masked blade, coated with TIKOTE-C from the midsection to the tip, was checked for coating thickness and the effects of the coating and coating thermal cycles on the base metal. A second blade, uncoated, was sectioned for comparison. Both blades had been previously tested in vibratory fatigue. The following significant observations were made in the course of the investigation:

1. The coating thickness on the first blade was measured in two areas: near the midsection (Section A) and near the tip (Section B). The results are shown in Figure 27. These dimensions do not include the thickness of the nickel plate, which was found to be 0.0005 in. throughout, except at the tip of the leading edge, where it was 0.0009 in.

(A) and (B) Voids at the Titanium/Nickel Interface. (C) Titanium Depleted Zone at the Tip of one Blade

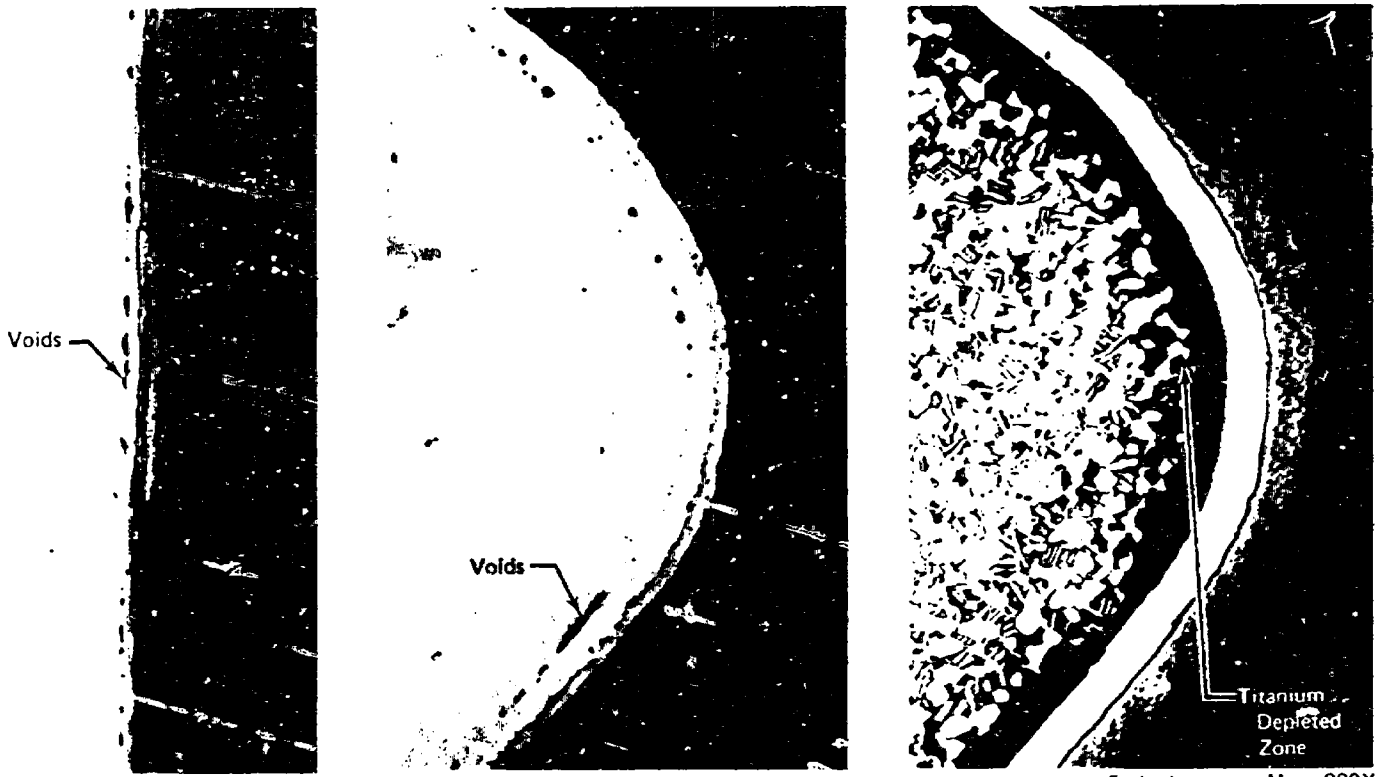

FAM 77958 Unetched Mag: 200X (A)

FAM 77955 Unetched Mag: 200X (B)

FAM 77956 Etched Mag: 200X (C)

Figure 37. Photomicrographs of PT6 A-27 Impeller Coated With TIKOTE®-C

FD 65133

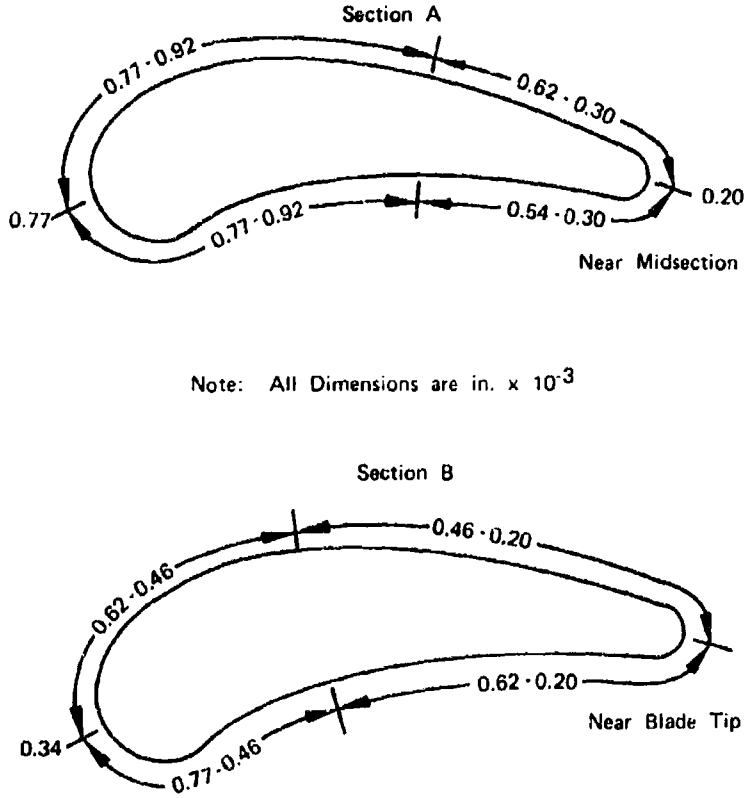

Figure 38. Cross Sections of JT8D Axial Compressor Blade Showing Thickness of TIKOTE®-C FD 65134

2. Voids were noted at the nickel/titanium interface throughout the blade (Figure 28), just as in the impeller examined previously.

3. In comparing the coated and uncoated blades, two major differences were observed. The normal $\alpha - \beta$ structure usually observed in the titanium alloy (Figure 29A, the uncoated blade) was transformed in the coated blade to the stabilized α structure, adjacent to the coating (Figure 29B). The remainder of the coated blade (further from the surface) had an enlarged grain structure (Figure 29C), which was attributed to the heat treatments involved in the coating application process.

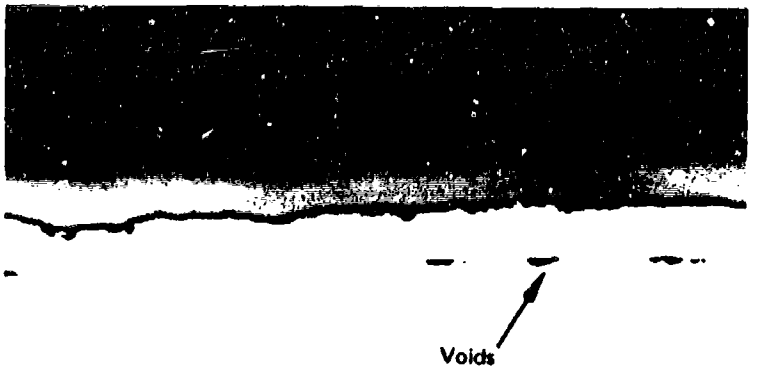

FAM 77849 Unetched Mag: 500X

Figure 39. Photomicrograph of JT8D 6th-Stage Compressor Blade Showing Voids at the Titanium/Nickel Interface. FD 65135

A coated JT8D blade with some TIKOTE-C overrun in the masked portion of the blade was examined to see if there was any nickel present under the TIKOTE-C. Light microscopy and X-ray diffraction showed no evidence of nickel under the TIKOTE-C coating in the overrun area. It was also noted that the coating did not appear to be tightly adherent to the titanium in this area.

(A) Normal α-β Structure, (B) Stablized α Structure, and (C) Enlarged Grain Structure

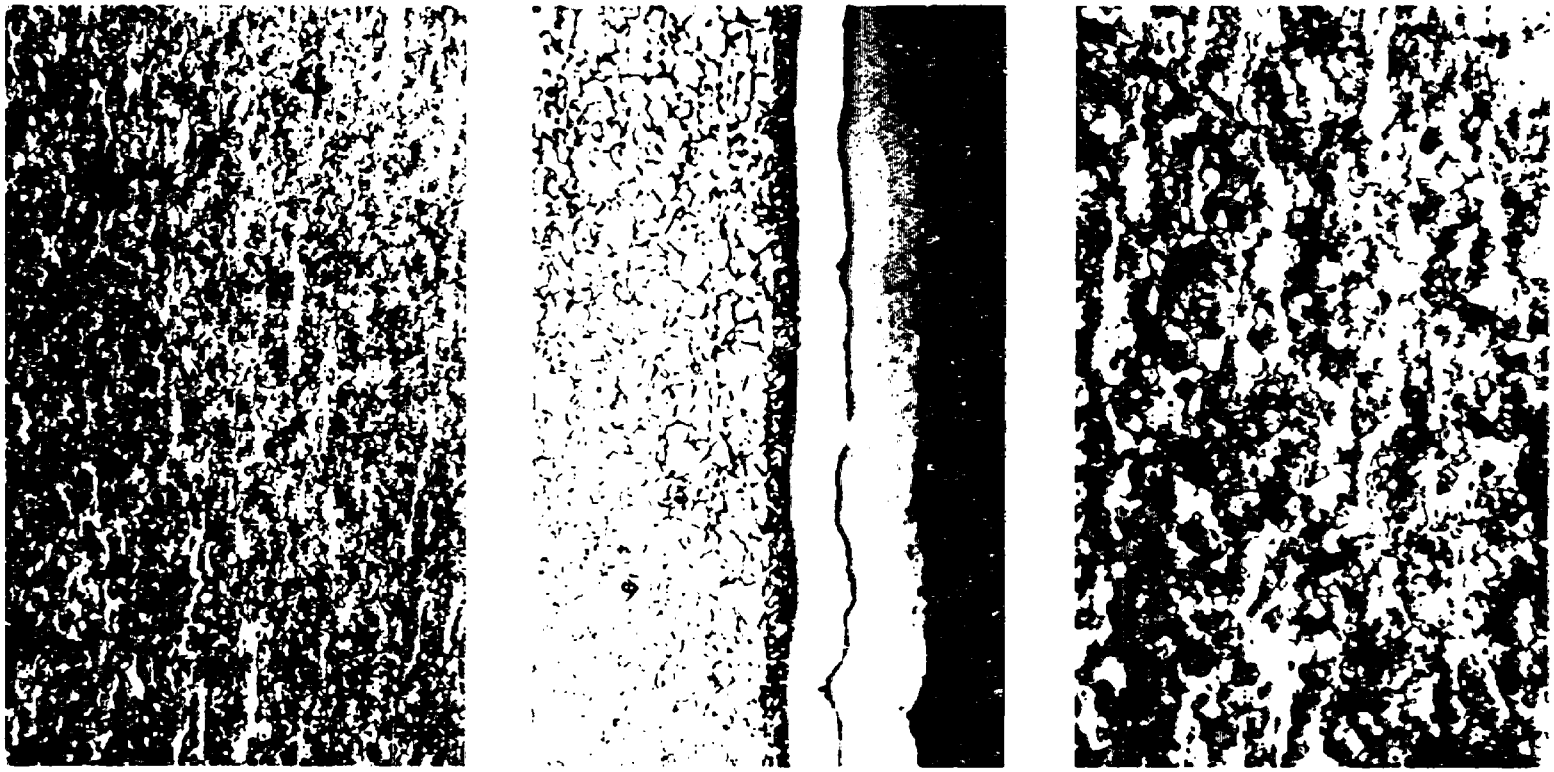

FAM 77854 Etched Mag: 500X (A)

FAM 77851 Etched Mag: 500X (B)

FAM 77852 Etched Mag: 500X (C)

Figure 40. Photomicrographs of JT8D 6th-Stage Compressor Blades Showing Microstructure Changes. FD 65136

CONCLUSIONS AND RECOMMENDATIONS

1. Texas Instruments, Inc., successfully demonstrated the ability to apply an adherent coating of TIKOTE-C to both titanium axial compressor blades and titanium centrifugal impellers from current production engines.

2. The goal of a uniform 0.001-in. thick coating was not achieved, but a sufficiently uniform coating of TIKOTE-C can be applied to wear-sensitive areas to provide a substantial increase in erosion resistance over bare titanium.

3. TIKOTE-C and titanium diboride coatings on nickel-plated Ti-6Al-4V alloy were 10 to 300 times more erosion resistant than uncoated titanium depending upon test conditions.

4. Both coatings were more erosion resistant at 20-deg angle of impingement than at 90-deg.

5. Application of TIKOTE-C to nickel-plated Ti-6Al-4V alloy does not seriously affect the tensile strength properties of the base metal, and somewhat improves the creep properties.

6. Rotating beam high-cycle fatigue tests indicate a reduction in fatigue life of over 60% for nickel plated specimens coated with both TIKOTE-C and with titanium diboride.

7. Coating the entire airfoil surface of axial compressor blades with nickel plating and TIKOTE-C reduces the first bending mode fatigue strength over 60%. However, masking the high stress areas to prevent adhesion of TIKOTE-C can result in no loss in usable fatigue strength.

8. Further evaluation is recommended to demonstrate the effectiveness of TIKOTE-C as an erosion-resistant coating in an engine environment by conducting a sand and dust ingestion test with coated titanium compressor components in a turboshaft engine used by the Army.

9. Further research is recommended to reduce the losses in fatigue strength, and to reduce the number of steps required to provide a satisfactory nickel plate interlayer.

APPENDIX I

STANDARD NICKEL PLATING PROCESS ON Ti-6Al-4V STR 169979

TEXAS INSTRUMENTS, INCORPORATED

STANDARD NICKEL PLATING PROCESS ON Ti-6Al-4V STR169979
TEXAS INSTRUMENTS, INCORPORATED

PROCESS PROCEDURE

1. Solvent clean - (acetone)
2. HF-HNO_3 dip - (1/2 to 2 min)
3. Tap water rinse - (quick dip)
4. Deionized water rinse
5. Citrate - HNO_3 dip - (5 min)
6. Tap water rinse - (quick dip)
7. Deionized water rinse
8. Ammonical electroless nickel - 50μ in.
9. Tap water rinse
10. H_2SO_4 dip (10 to 20% vol)
11. Tap water rinse
12. Sulfamate nickel plate - 50μ in.
13. Tap water rinse
14. Dry - Isopropyl alcohol and clean compressed air - (white glove handling)
15. Heattreat at 1200°F for 30 min in a clean vacuum oven and oven cool
16. Solvent clean - (acetone)
17. Vapor hone, if required
18. Tap water rinse
19. Activate (fresh 50% vol HCl); (time - till gassing)
20. Wood's nickel strike
21. Tap water rinse
22. H_2SO_4 dip - (10 to 20% vol)
23. Tap water rinse
24. Sulfamate nickel plate - 150μ in.
25. Tap water rinse
26. Dry - Isopropyl alcohol and clean compressed air - (white glove handling)
27. Heattreat at 950°F for 30 min in a clean vacuum oven and oven cool

APPENDIX II

LISTING OF EROSION COATING RUNS

Run Serial No.	Sub-strate	Substrate Prepa-ration	Tem-per-ature, °C	Run Time, hr	Coating Thickness/ Rate, 0.001 in./hr	Results: Adhesion	Results: Coating Hard-ness, KHN 25	Results: Erosion Resist-ance	Results: Sub-strate Ductility
2441-1	Ti-6Al-4V	Sulfamate Ni on E/Ni	630*	0.8	0.5-0.6/0.7	Some failure between Ni layers; TI-KOTE®C adhesion good; substrate structure affected for ~1.5 mil from interface			
2451-1	Ti-6Al-4V	Sputtered TI-KOTE®C	618	1.4	1.3/0.9	Bond only fair between TI-KOTE®C layers; substrate underneath was practically unaffected			
2591-1	Ti-6Al-4V	Sputtered Ni on sputtered Mo and sputtered TI-KOTE®C on sputtered Mo	635	1.5	1.2-1.3/0.8	Nickel sample some failure at titanium interface. Titanium structure affected ~0.8 mils; TI-KOTE®C sample - bond appeared good, substrate appeared unaffected		Good	Good
2591-2	Ti-6Al-25n-42r-2Mo	Sputtered Ni on sputtered Mo	630	1.5				Good	Fair

Run Serial No.	Sub-strate	Substrate Prepa-ration	Tem-per-ature, °C	Run Time, hr	Coating Thickness/ Rate, 0.001 in./hr	Results: Adhesion	Results: Coating Hard-ness, KHN 25	Results: Erosion Resist-ance	Results: Sub strate Ductility
2671-1	Ti-6Al-4V	Sputtered Ni on sput-tered Mo	633	1.5	1.0/0.7	Bond appeared good; substrates structure slightly affected ~0.8 mils		Good	Good
2741-1	Ti-6Al-4V	Sputtered Ni on sput-tered Mo	615	1.5	0.6/0.4	Bond appeared good; substrate structure slightly affected ~0.2 mils	2642	Good	Good

Run Serial No.	Substrate Preparation	Temperature, °C	Run Time, hr	Coating Thickness/Rate, 0.001 in./hr	Results: Adhesion	Results: Coating Hardness, KHN 25	Results: Erosion Resistance	Results: Substrate Ductility
1371-1	Watts Ni Plate	680	1.5	-	Ni blistered coating adhered well to Ni			
1441-1	Ni plate	675	1.3	-	-			
1801-1	Ni plate	645	1.5	-	Visually good			
1831-1	Sputtered Ni	635	1.0	1.1/1.1	Fair	2995		Poor
2101-1	Sulfamate Ni	630	0.67	-	Visually good			Fair to poor (dependent preparation)
2171-1	Sputtered Ni	630	1.16	0.9/0.78	Part visually good, part flaked either within the Ni layer or at the Ni-TI-KOTE®C interface	3107		
2231-1	Sulfamate Ni on sputtered Ni	625	1.0	0.7/0.7	TI-KOTE®C adhesion good, but Ni failed between layers	3227		
2251-1	Ni plate (outside vendor)	1.0	1.0	0.75/0.75	Very good	2555		Fair

Run Serial No.	Substrate Preparation	Temperature, °C	Run Time, hr	Coating Thickness/Rate, 0.001 in./hr	Results: Adhesion	Results: Coating Hardness, KHN 25	Results: Erosion Resistance	Results: Substrate Ductility
2311-1	Thick Sputtered Ni	620	1.3	0.6/0.46	Visually good, but flaked in the Ni layer when sectioned	2837		
2311-1	Sputtered TI-KOTE®C	620	1.3	-	Poor (sputtered material appeared powdery)	-		Good
2351-1	Ni plate and vac bake	630	1.5	1.2/0.8	Visually good, Ni appears layered, but continuous	2995		Good
2381	Sputtered TI-KOTE®C	625	1.25	1.4/1.1	Partial bond failure at thin layer between two TI-KOTE®C layers	2837		Very good

Run Serial No.	Substrate Preparation	Temperature, °C	Run Time, hr	Coating Thickness/Rate, 0.001 in./hr	Results	Coating* Erosivity, sec/0.001 in.
3061-1[1]	Sputtered Ni	665 (in hot area)	1.33	Varied from 7.08 to 0.3		
3091-1[1]	Sputtered Ni	620	2.0	1.2/6		
3121-1[1]	Electroplated Ni	630	2.0	1.0/0.5		
3131-1[1]	Electroplated Ni	620	2.0	-		
3151-1[1]	Sputtered Ni	625	2.0	1.2/0.6		
3201-1[1]	Sputtered Ni	625	1.0	-		
3221-1[3]	(a) Sputtered Ni	630	1.0	0.6/0.6		
	(b) Sputtered Ni	630	1.0	0.7/1.7		
3281-1[2]	Sputtered Ni	630	1.0	0.65/0.65		
3351-1[1]	Electroplated Ni	630	1.5	0.9/0.6		
3351-1[2]	Sputtered Ni	630	1.5	-		

Run Serial No.	Substrate Preparation	Temperature, °C	Run Time, hr	Coating Thickness/Rate, 0.001 in./hr	Results	Coating* Erosivity sec/0.001 in.
3132-4(I)**	Glass bead peened	665	4.0	1.2-2.7 / 0.3-0.7		
3231-4(I)**	P&WA Process	665	3.0	-		
3331-4(1)	TI Electroplated Ni	665	3.0	0.5-1.8 / 0.2-0.6		

**Flows as follows:

N_2 through $TiCl_4$	= 27 l/min
N_2	= 56 l/min
H_2	= 10 l/min
Anion	= 0.3 l/min

Run Serial No.	Substrate Preparation	Temperature, °C	Run Time, hr	Coating Thickness/Rate, 0.001 in./hr	Results: Adhesion	Coating* Erosivity, sec/0.001 in.
2781-1(1)	Sputtered Ni	625	1.8	1.1-1.2/0.65	Poor adherence of sputtered coating to the substrate; flaked badly when bent.	
2791-1(2)	Sputtered Ni	615	1.75	0.9/0.51	Some flaking on edge of one coupon, otherwise good.	
2861-1(2)	Sulfamate Ni on electroless Ni	630	1.5	1.0/0.67	Appeared good in mount.	
2931-1(1)	Sulfamate Ni on electroless Ni	630	2.0	1.3/0.65	Visually looked good; no flaking or chipping.	600
2991-1(1)	Sulfamate Ni on electroless Ni	630	1.5	0.6-0.7/0.42	Some chipping on edges of two coupons; generally good.	1500
3001-1(1)	Sulfamate Ni on electroless Ni	630-650	immediate shutdown due to sample discoloration			
3001-1(3)	Sputtered Ni	625	2	1.2-1.5/0.9	One coupon flaked badly on 25% of the coupon; rest of run quite good.	1500
3011-1(2)	(2) Sputtered Ni	(a) 630	2	1.1-1.3/0.6	(a) Looks good	500
	(6) Sputtered Ni	(b) 625	2	1.1-1.4/0.63	(b) Some chipping and flaking on edges	1000

*Compared with Ti-6Al-4V at 35 sec/1 mil

Run Serial No.	Substrate Preparation	Temperature, °C	Run Time, hr	Coating Thickness/Rate, 0.001 in./hr	Results
0402-1[1]	Electroplated Ni	635	1.5	0.4-0.6/0.33	Looked good, except alkaline etched
0472-1[1]	Blades	~635	1.5	-	Looked good
0592-1[1]	Sputtered	660	2.0	0.8-1.0/0.45	Flaked
0592-1[2]	Sputtered (fatigue bars)	645	1.5	0.7/0.47	Flaked
0602-1[1]	Electroplated (fatigue bars)	645	1.5	-	Looked good
0602-1[2]	Electroplated (fatigue bars)	640	1.5	-	Looked good
0542-3[1]	Electroplated (impeller)	640-670	3.5	-	Looked good
0212-1[1]	Sputtered Ni	630	1.0	0.4-0.6/0.5	

Run Serial No.	Substrate Preparation	Temperature, °C	Run Time, hr	Coating Thickness/Rate, 0.001 in./hr	Results	Coating* Erosivity, sec/0.001 in.
0612-1(1)	E/L plated Ni coupons	640	1.5	1.2	Looked good	
0612-1(2)	Sputtered Ni blades	630-660 (middle - mid position to blade tip)	1.5	0.1-0.7 (thin on edges)	Visually looked good	
0632-1(1)	Sputtered Ni coupons	640	1.5		Flaked on coupon edges	
0762-1(1)	-	-	-	-	Heating tests for blade heating profile	
0762-3(1)	-	-	-	-	Heating tests for blade profile	
0812-1(1)	Electroless Ni coupons	650	1.0	-	Coating flaked	
0902-1(1)	Electroless Ni	650	1.0	-	Coating flaked	
0982-1(1)	Electroless Ni coupons	630	1.5	-	Coating flaked	
1022-1(4)	Vac baked borane El/$_{Ni}$+Sulf Ni	660	1.5	-	Flaked	
1022-1(4)	Vac baked borane El/$_{Ni}$	650	1.5	-	Flaked	

Run Serial No.	Substrate Preparation	Temperature, °C	Run Time, hr	Coating Thickness/Rate, 0.001 in./hr	Results	Coating* Erosivity, sec/0.001 in.
1022-1(4)	Vac baked borane El/Ni (slow rate)	630	1.5	-	Flaked	
1022-1(4)	Borane El/Ni+Sulf-Ni	640	1.5	-	Flaked	
1022-1(4)	Borane El/Ni	660	1.5	-	Flaked	
1022-1(4)	Borane El/Ni(slow rate)	650	1.5	-	Flaked	
1332-1(1)	Bare Ti-6Al-4V fatigue bars	650	1.5	-	Flaked	
1332-1(2)	Bare Ti-6Al-4V fatigue bars	660	1.5	-	Flaked	
1362-1(1)	Bare Ti-6Al-4V bolts	670	1.5	-	Flaked	
1362-1(3)	-	-	-	-	Heating profile tests on TI blades	
1372-1(1)	-	-	-	-	Heating profile tests on TI blades	
1382-1(1)	Sulfamate Ni fatigue bars	660	1.5	-	Good adhesion on Ni plated portion	

Run Serial No.	Substrate Preparation	Temperature, °C	Run Time, hr	Coating Thickness/ Rate, 0.001 in./hr	Results	Coating* Erosivity, sec/0.001 in.
1392-1(1)	Sulfamate Ni fatigue bars	675	1.5	-	Ni plated all over; adhesion good	
1392-1(2)	Bond strength specimen - sulfamate Ni plated	665	1.5	-	Looked good	
1402-1(1)	Stress corrosion coupons	-	-	-	Heating tests	
1432-1(1)	Erosion coupons - sulfamate Ni plated	655	1.75	-	Looked good	
1432-1(2)	Erosion coupons	660	1.75	-	Looked good	
1432-1(3)	Over lap shear coupons Sulf-Ni	655	1.5	-	Looked good	
1442-1(1)	Stress corrosion	640	1.75	-	Some looked good, some didn't	
1452-1(1)	Tensile bars	660	1.75	-	Parts looked good	
1452-1(2)	Creep bars	670	1.75	-	Looked good	
1452-1(3)	Fatigue bars Sulf-Ni	660	1.75	-	Looked good	
1462-1(1)	Fatigue bars Sulf-Ni	660	1.75	-	Parts flaked	

Run Serial No.	Substrate Preparation	Temperature, °C	Run Time, hr	Coating Thickness/Rate, 0.001 in./hr	Results	Coating* Erosivity, sec/0.001 in.
1462-1(2)	Fatigue bars Sulf-Ni (thick)	650	1.75	-	Parts looked good	
1442-3(1)	Impeller Sulf-Ni (with anode fixture)	660	3.5	-	Looked good	
1522-1(1)	Small blades E/L Ni	630	1.25	-	Looked good	
1542-1(1)	Large blades E/L Ni	665	1.75	-	Looked good	
1542-1(2)	Large blades E/L Ni	660	1.75	-	Looked good	
1572-1(1)	Large blades E/L Ni	660	1.75	-	Looked good	
1572-1(2)	Large blades E/L Ni	660	1.75	-	Looked good	
1602-1(1)	6-in. Ti tubes	Study heating profile			-	
1602-1(2)	Scrap Ti PT6 blades	Study heating profile			-	
1612-1(1)	PT6 blades stage I E/L Ni	660	1.75	-	Looked good	

APPENDIX III

METHOD FOR DETERMINING COATING ADHESION BOND STRENGTH IN SHEAR

METHOD FOR DETERMINING COATING ADHESION BOND STRENGTH IN SHEAR

1. Apparatus

   1.1 AMS 4911 titanium alloy coupons approximately 1- by 4- by 0.125-in. thick and coated with TIKOTE®-C

   1.2 Tensile testing machine - 5000-lb capacity minimum.

2. Procedure

   2.1 Preparation of test specimen

      2.1.1 Degrease coated coupon with acetone

      2.1.2 Dry coupon in clean air or nitrogen blast

   2.2 Bonding with PWA 592 nylon epoxy bonding film

      2.2.1 Place 0.5-in. by 1-in. piece of bonding film on the end of one coupon

      2.2.2 Overlap second coupon end by exactly 0.5-in., and fixture with glass tape, so that movement between coupons is minimized

      2.2.3 Apply a uniform, constant pressure of 50 psi $\mp$ 5 to the area to be bonded

      2.2.4 Cure film at 350 °F $\mp$ 5 for 1 hr

      2.2.5 Cool specimen below 200 °F before releasing pressure

   2.3 Bond Strength

      2.3.1 Pull properly fixtured specimen in tension at 0.05 in./min crosshead speed, record load

      2.3.2 Shearing at coating/substrate interface is a measure of bond strength

      2.3.3 Measure length and width of bonded area to the nearest 0.01 in. and record

3. Recording and Reporting

$$\text{Shear Strength} = \frac{\text{Load Required for Separation}}{\text{Length by Width of Overlap}}$$

APPENDIX IV

METHOD FOR DETERMINING COATING ADHESION BOND STRENGTH IN TENSION

METHOD FOR DETERMINING COATING ADHESION BOND STRENGTH IN TENSION

1. Materials

   1.1 Adhesive: Scotchweld EC-2186 one-component epoxy (3M Co.).

   1.2 Specimen: AMS 4928 machined according to Figure 1.

   1.3 Solvent: Acetone PMC 9008.

   1.4 Bonding Fixture: Spring, threaded rod, nuts, washers.

2. Procedure

   2.1 Prepare specimen

      2.1.1 Vapor blast the bonding surfaces of the coated test specimen and an identical unplated specimen.

      2.1.2 Rinse thoroughly in cold water.

      2.1.3 Rinse in acetone.

      2.1.4 Air dry.

   2.2 Bond specimen

      2.2.1 Apply a uniform 5- to 10-mil coating of adhesive to the end of each specimen.

      2.2.2 Assemble specimen halves per Figure 2.

      2.2.3 Cure adhesive at 350°F ± 5 for 1 hr.

      2.2.4 Remove bonding fixture.

   2.3 Pull specimen on tensile machine

      2.3.1 Fixture specimen on tensile machine and pull at cross head speed of 0.05 in./min.

      2.3.2 Record ultimate tensile load in pounds.

3. Calculations

   3.1 Compute bond strength.

$$\text{Bond Strength, psi} = \frac{\text{Ultimate tensile load, lb}}{\text{Bonded area, in}^2}$$

FIGURE 1

BOND STRENGTH SPECIMEN

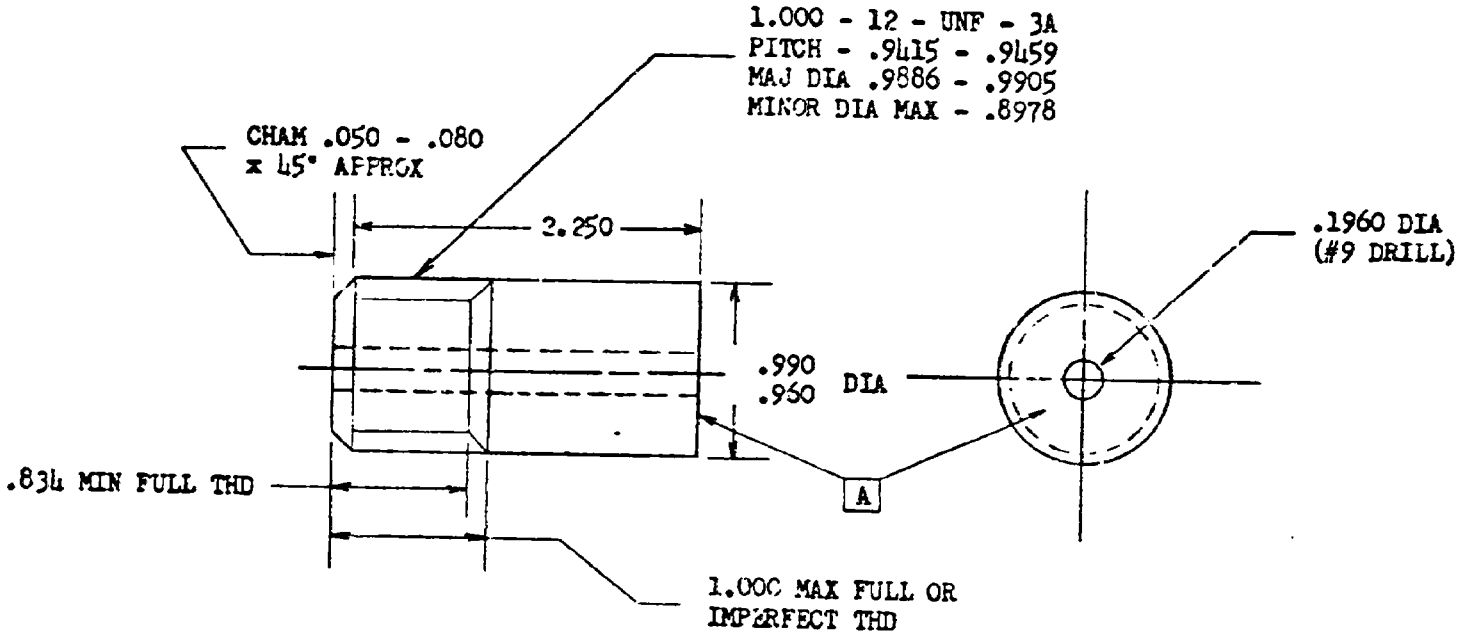

(1) SURF [A] MUST BE SQUARE WITH CENTERLINE WITHIN .001 FIR BEFORE COATING

(2) DRAWING NOT TO SCALE

W.J.G.
1/10/72

FIGURE 2

ASSEMBLED SPECIMEN HALVES

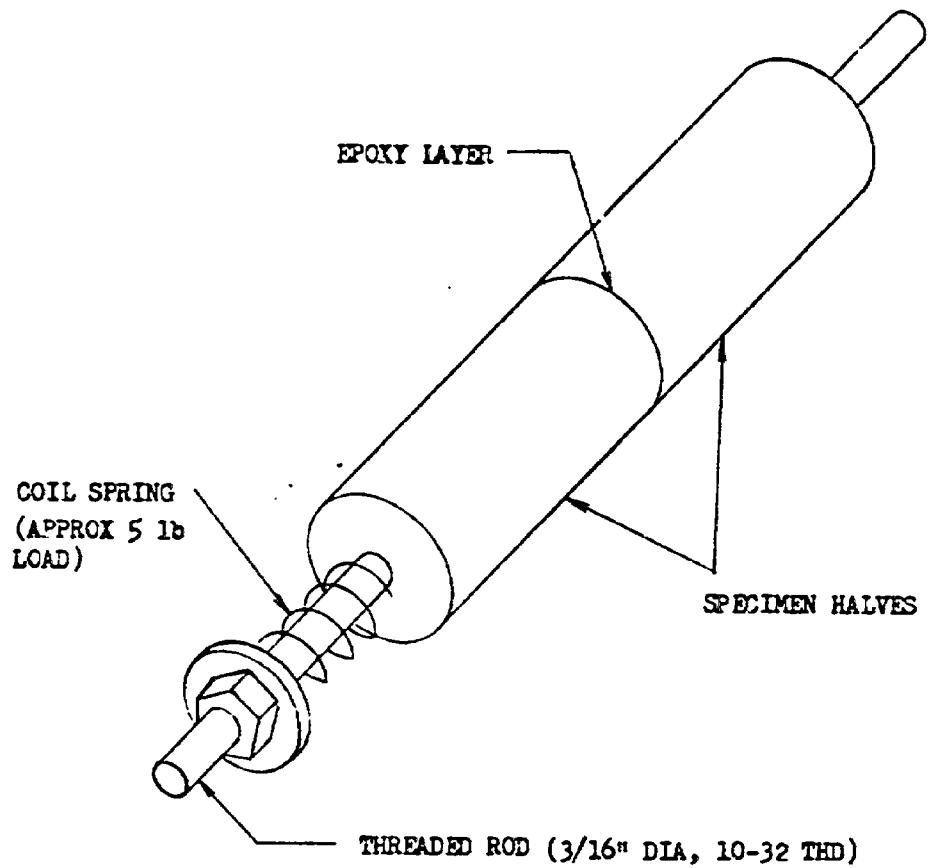

W.J.G.
1/10/72

APPENDIX V

METHOD FOR DETERMINING THE EFFECTS OF HOT SALT STRESS CORROSION ON TITANIUM ALLOYS

DETERMINATION OF THE EFFECT OF MATERIALS & PROCESSES ON STRESS CORROSION OF TITANIUM ALLOYS

1. SCOPE

This section describes the procedure for determining the effect of materials and processes on stress corrosion titanium test pieces.

2. APPARATUS

2.1 Stress Corrosion Test Specimens: AMS 4916 sheet, 5.741 ± 0.005 in. long, 0.032 ± 0.001 in. thick, 0.5 ± 0.1 in. wide.

2.2 Specimen Holder: Refer to Figure 1.

2.3 Oven: Circulating air, capable of heating to and maintaining 900°F ± 10 for 100 hours.

2.4 Microscope: Capable of 10X magnification.

2.5 Microsyringe: Capable of measuring 50 ± 5 microliters.

2.6 Sodium Chloride Solution: 3% aqueous solution of sodium chloride prepared with distilled or demineralized water.

3. PROCEDURE

3.1 For PWA™ 36 Electroless Nickel or PWA 37 Anodic Treatment

3.1.1 Clean the test specimens (anodized) and a control specimen (not treated) with acetone. Use white gloves or the equivalent when handling specimens to prevent contamination.

3.1.2 Bend the test specimens and one control specimen into the specimen holder.

3.1.3 Place 50 ± 5 microliters of 3% sodium chloride solution from a microsyringe onto an approximately one inch long section of each specimen. The solution should be placed near the center and on the convex side of the specimens.

3.1.4 Dry at 180 - 200°F. A solid residue shall remain on the specimens.

3.1.5 Place the holder with the specimens into a clean circulating air oven at 900°F ± 10 for 100 hours.

3.2 For All Other Surface Treatments

3.2.1 Clean a control specimen (not treated) with acetone. Use white gloves or the equivalent when handling specimens to prevent contamination.

3.2.2 Bend the test specimens treated with the material or process being tested and one control specimen into the specimen holder.

3.2.3 Place the holder with the specimens into a clean circulating air oven at 900°F ± 10 for 100 hours.

4. EXAMINATION

4.1 Examine the specimens at 7 - 10X for breaks or obvious cracks while they are still in the specimen holder.

4.2 Test is invalid if control specimen does not break or show obvious cracks. Repeat all tests using new control and test specimens.

4.3 If control or test specimen shows no breaks or cracks, remove from the holder and treat as follows.

4.3.1 Vapor blast the specimen.

4.3.2 Immerse the specimen into a solution of: 5 parts nitric acid, one part hydrofluoric acid and one part sulfuric acid at 130 - 150°F for 30 seconds or until excessive red fumes are liberated, whichever comes first.

4.3.3 Immediately rinse the specimen in running water and dry.

4.3.4 Examine the specimen at 7 - 10X for cracks.

5. RECORDING AND REPORTING

5.1 Test Specimen Showing Breaks or Cracks: Record and report, "Test specimens treated to MCL Manual Section K-231, and examined per paragraph 4.1 (or 4.2) show evidence of breaks or cracks. Test specimens fail to pass the stress corrosion test."

5.2 Test Specimen Showing No Evidence of Cracks: Record and report, "Test specimens pass the stress corrosion test per MCL Manual Section K-231."

5.3 Control Specimen Shows No Evidence of Cracks: Record, "Test not valid. Control specimens show no evidence of cracks."

FIGURE 1 SPECIMEN HOLDER
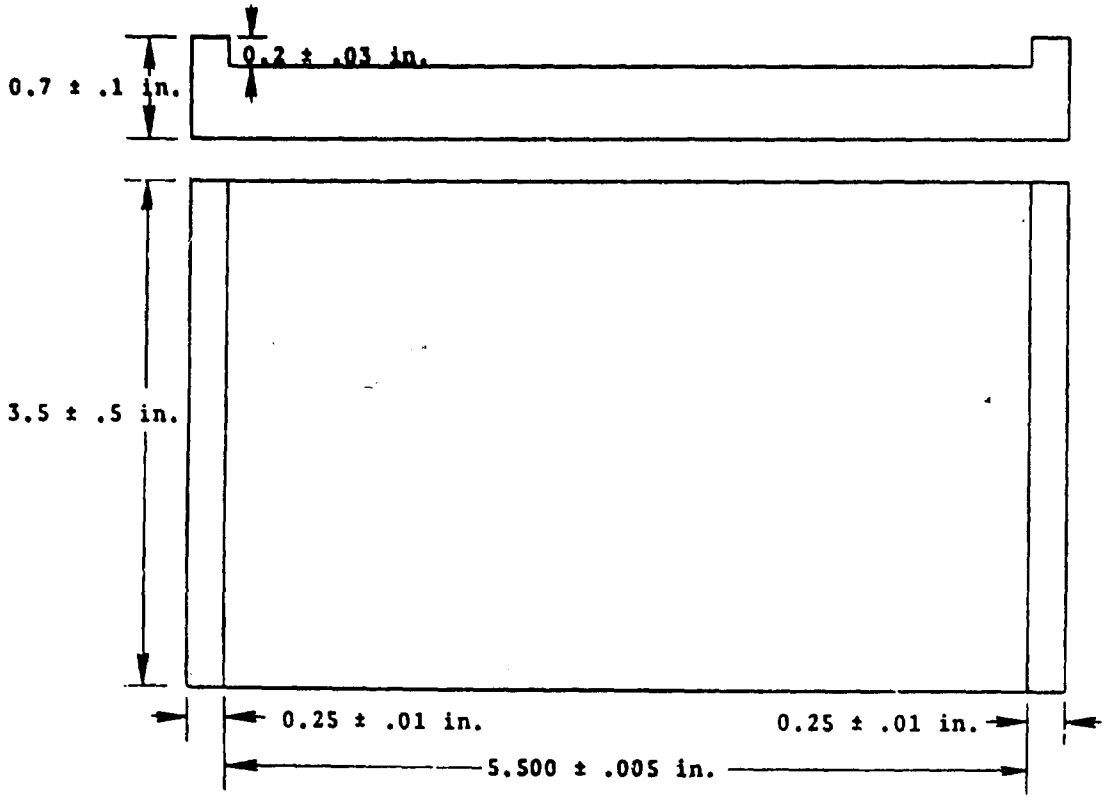
Material: Nickel Base Alloy or Nickel Plated, Type 300 Series Stainless Steel. Finished Dimensions After Plating.